Supplementary Information Appendix (SI Appendix)

Supplementary Results

The presence of SUF – Fe/S cluster assembly system in *Blastocystis* sp.

We identified partial sequences of genes homologous to the bacterial and plastid SufC and SufB proteins amongst the *Blastocystis* ESTs. In our effort to amplify full-length genes using RACE, we discovered that both genes appeared to be transcribed on one mRNA encoding a single open-reading frame (ORF) with the *sufC* homologous region upstream of the *sufB* segment. We confirmed this by amplifying a full-length *Blastocystis SufCB* gene from both genomic DNA and cDNA. The presence of 10 canonical spliceosomal introns (with GT - AG splicing boundaries) in the genome but not the cDNA (**Fig. S1**) shows that this sequence is not derived from a bacterial or archaeal contaminant. Although the *Blastocystis* SufCB protein is the first known example of this pair of SUF components fused into a single polypeptide, this domain arrangement is tantalizingly similar to the structure of the SUF operon with *sufC* followed by *sufB*, found in a restricted set of genomes of anaerobic and/or thermophilic Bacteria and archaea that contain the putatively 'primitive' SUF system (**Fig. S2**) (1).

The *Blastocystis* SUF protein possesses distinctive sequence and structural properties characteristic of methanoarchaeal homologs

The SufC domain of the *Blastocystis* SufCB protein possesses the ABC ATPase signatures including the Walker A and B boxes as well as the Q-,P-,D- loops and the H-

motif, which are characteristic for all the representatives of this family (**Fig. S21**). No potential transmembrane segments were predicted for this domain using TMHMM v2.0 (2), despite its clear homology to the ABC transporter family. Interestingly, at the C-terminal end, *Blastocystis* SufC domain sequence retains a CX_nCX_2C motif that is present neither in *E. coli* SufC, nor in other bacterial homologs, but is conserved in the SufC of several Methanoarchaea, *Caldidecellulosiruptor, Dehalococcoides* spp and δ-proteobacteria; this motif might function as a metal binding site.

The *Blastocystis* SufB domain and its Methanobacteriales orthologs (**Fig. S9**) are missing a number of features shared by *E. coli* and other bacterial homologs, The *E. coli* SufB protein contains the flavin adenine dinucleotide **(**FAD) binding motifs (3), that are absent from both *Blastocystis* as well as from Methanomicrobiales and also from *Dehalococcoides*, δ-proteobacteria and Thermatogae (see **Fig. S5** for details). In addition, conserved cysteine residues that are found in *E. coli* and *E. chrysanthemi* homologues (especially at the C-terminal of the protein) are also absent from *Blastocystis* and the Methanomicrobiales but also from *Dehalococcoides*, δ-proteobacteria, Thermatogae, Actinobacteria and Firmicutes (see **Fig. S9** for details). The presence of the CX_nCX_2C motif in SufC and the lack of the FAD binding motifs in SufB are distinctive sequence features that *Blastocystis* shares with the Methanomicrobiales, which strengthen the LGT hypothesis for the origin of the *Blastocystis* SufCB protein. However, these differences from the well-characterized SUF proteins also raise questions about the *in vivo* function of these proteins.

Blastocystis SufCB was acquired from an anaerobic archaeon by lateral gene transfer

The discovery of the *sufCB* gene in *Blastocystis* was unexpected as the *sufC* and/or *sufB* genes have, until now, only been found in the genomes of plastid-bearing eukaryotes (4). Since the ancestor of all stramenopiles is hypothesized to have acquired plastids derived from a secondary red-algal endosymbiont early on (5), one possible explanation for *sufCB* in *Blastocystis* is that it derives from an ancestral (or existing vestigial) plastid in this lineage. Alternatively, *Blastocystis* may have independently gained the *sufCB* gene from a recent lateral gene transfer (LGT) from another photosynthetic eukaryote, a bacterium or an archaeon. To distinguish between these scenarios, we mined the various genomic and EST sequence databases from available eukaryotes and representative bacterial and archaeal groups to construct a comprehensive alignment of homologous sequences. Maximum likelihood (ML) and Bayesian phylogenetic analyses of the SufB homologs grouped the *Blastocystis* sequence specifically within a group composed of methanoarchaea and miscellaneous anaerobic bacteria, with strong bootstrap support and posterior probability placing it as a sister group to Methanomicrobiales (**Fig. S3**). The SufC protein phylogenies showed a similar general grouping, although the position of the *Blastocystis* homolog was only weakly supported (**Fig. S4**). To enhance phylogenetic resolution we concatenated the two protein datasets. ML and Bayesian analyses of the larger dataset showed a strongly supported (ML bootstrap = 95, PP = 1.0) sister-group relationship between the *Blastocystis* SufCB and the Methanomicrobiales (**Fig. 1 and Fig. S5**), and that this lineage emerged from within a grouping of homologs from anaerobic and/or thermophilic archaea and bacteria.

Notably, these sequences were all well separated from the clade of plastid homologs from various photosynthetic eukaryotes, including other stramenopiles that clustered with their cyanobacterial relatives. To formally test that the *Blastocystis* sequences had a separate origin from the stramenopile plastid group, we used three statistical topology tests, the Approximately Unbiased (AU), Kishino-Hasegawa (KH), and Shimodaira-Hasegawa (SH) tests implemented in CONSEL (6). The ML tree (**Fig. S5**) was compared to a topology where all eukaryotic plastid homologs plus *Blastocystis* were constrained to be monophyletic (**Fig. S5**). The monophyly of *Blastocystis* and eukaryotic plastid homologs was rejected by all three tests (AU-test p-value = 0.01, KH-test p-value= 0, SH p-value= 0). The simplest explanation of this phylogenetic pattern is that *Blastocystis* acquired the *sufCB* operon via LGT from an archaeon from within, or related to, the order Methanomicrobiales, with subsequent fusion of both genes into a single ORF.

SufCB functions in the cytoplasm of *Blastocystis*

An antibody raised against *Erwinia chrysanthemi* SufC (7) showed clear specificity for a protein of the size predicted for *Blastocystis* SufCB (~77 kDa) in western blot analysis of both *Blastocystis* total cell lysates and *E. coli* heterologously expressing the above protein (**Fig. S10a**). Confocal immunofluorescence microscopy using this antibody showed a strong but diffuse labeling distribution indicating a cytoplasmic location of SufCB in *Blastocystis* (**Fig. 2a-f**), consistent with the western blot analysis of the same antibody in different subcellular fractions of *Blastocystis* proteins (**Fig. S10e**). There was no overlap with the Mitotracker signal labeling MROs and very little if any signal co-localized with the central vacuole (**Fig. 2c & 2e**). To visualize the localization

of the anti-SufC antibody at a higher resolution we employ immunogold labelling and electron microscopy (EM). Transmission EM revealed an abundance of gold particles in the cytosol and their virtual absence from the MRO and the vacuole (**Fig. 2g & S11**). Statistical analysis of the density of the gold particles per μm^2 of the cytosol relative to MRO and other compartments of the cell suggests that SufCB is confined to the cytosol (**Fig. 2h**). Non-specific binding of the gold-conjugated secondary antibody was excluded by performing the same experiment using only the secondary antibody as a control. Collectively, the immunomicroscopy data convincingly demonstrate that *Blastocystis* SufCB protein is abundantly expressed in the cytoplasm of the parasite.

The *Blastocystis* genome encodes proteins of the ISC and CIA systems

To fully delineate the makeup of the ISC system of *Blastocystis* we sought genes encoding proteins known to play pivotal roles in the *Saccharomyces cerevisiae* mitochondrial ISC machinery (**Table S1**). To do this, we used BLAST and the HMMER profile methods to search an 'in-house' *Blastocystis* transcriptomic (expressed sequence tag: EST) sequence database (8) using the *S. cerevisiae* ISC protein components as queries. Essential ISC components that were not found in this way were targeted by a degenerate PCR approach using *Blastocystis* genomic DNA and complementary DNA (cDNA) as templates. In total, we identified homologs of ten of the ISC system components including *iscU*, *iscS*, frataxin (*yfh1*), *mrs3/4*, ferredoxin (*yah1*), mitochondrial *hsp70*, *mge1*, *jac1*, glutaredoxin (*grx5*) and *isa2*. We also identified an incomplete putative mitochondrial Fe/S cluster-exporting *atm1* homolog. Similarly, we identified genes that encode members of the CIA machinery such as *cia1, nbp35* and

nar1 in the EST database. For genes where the full-length coding sequence was not available in the EST data, a full-length coding region was obtained using 5' and 3' rapid amplification of cDNA ends (RACE) and gene-walking techniques. *In silico* predictions identified canonical N-terminal targeting signals on some of the ISC proteins indicating that they may be targeted to the MRO of *Blastocystis* (**Table S1**). Like their yeast orthologs, *Blastocystis* CIA proteins were not predicted to posess organellar targeting signals (**Table S1**), indicating their probable cytosolic location.

Blastocystis ISC and CIA proteins possess conserved residues that are known to be structurally and functionally important.

The full-length amino acid sequences of *Blastocystis* IscS, IscU and frataxin were aligned with selected prokaryotic and eukaryotic ISC proteins (**Fig. S13 – S15**). The key amino acid residues required for the functionality of these proteins in several organisms (IscS: residues involved in substrate binding and function; IscU: residues forming the iron binding site and responsible for the functional interaction with Hsp70; Frataxin: candidate iron-binding residues) are conserved in the *Blastocystis* homologues, suggesting they do function in an ISC system in this organism. As a representative of the CIA machinery, the full-length amino acid sequence of the putative *Blastocystis* Nbp35 was aligned with other eukaryotic homologs in order to demonstrate that it too retains functional domains (including Walker A and B motifs, and cysteine residues) characteristic for this protein family (**Fig. S22**).

The _Blastocystis_ ISC components function within mitochondrion-related organelles

To experimentally determine the localization of the ISC machinery within *Blastocystis,* we selected key components that are considered vital for ISC function in yeast: the scaffold assembly protein IscU, the cysteine desulfurase IscS and the putative ferrous iron donor, frataxin. Antibodies raised against *Trichomonas vaginalis* IscS (9), *Giardia intestinalis* IscU (10) and *Trypanosoma brucei* frataxin (11) show clear specificity for proteins of the expected size of *Blastocystis* homologs (50.8 kDa, 16.3 kDa and 16.9 kDa for IscS, IscU and frataxin respectively) in total cell extracts (**Fig. S10 b-d**). Confocal immunofluorescence microscopy of *Blastocystis* cells labeled with these antibodies showed, in all three cases, a strong signal for the labeled proteins that co-localized with the mitochondrion-specific dye MitoTracker (**Fig. 4** and **Fig. S12**). This pattern indicates that counterparts of the mitochondrial ISC machinery in *Blastocystis* function within its MROs.

Supplementary Materials and Methods

Blastocystis culturing

Blastocystis NandII was cultured on egg media slants as described by Zierdt and colleagues (12). Cultures were maintained at 37 °C within an anaerobic chamber (80% nitrogen, 10% hydrogen, 10% carbon dioxide) and transferred to fresh media every 5 days.

Protein sequence analysis and bioinformatic predictions

To identify candidate ISC pathway proteins we used CBorg (13) a comparative BLAST tool for organelles. Full-length sequences of the genes encoding proteins, were determined by manual inspection and BLASTX (14) searching to identify the protein coding regions by database search similarity (15). The *Blastocystis* amino acid sequences were then aligned with homologous sequences from bacteria and other eukaryotes using ClustalX (16). The secondary structure of the proteins were predicted using a combination of PSIPRED (17) and HMMTOP (18). The transmembrane topology for the proteins was predicted using TMHMM v3 (19). For the *in silico* prediction of potential mitochondrion-targeted proteins we employed Mitopred (20) Mitoprot (21), Predotar (22) and TargetP (23).

Immunoblotting

Protein samples were heated at 96 °C for 10 min and centrifuged at 13,000 x g for 5 min. Samples were loaded on to an acrylamide gel and proteins were resolved via sodium dodecyl-sulfate polyacrylamide gel electrophoresis (SDS-PAGE). Proteins were transferred to Immuno-Blot polyvinylidene difluoride (PVDF) membranes (BioRad), visualized by Pounceau staining and then were blocked for an hour with 1% skimmed milk in TBS-tween (0.1%). Membranes were washed with 0.5% skimmed milk in TBS-tween (0.1%) three times for 10 min. The primary antibody was diluted in 1% skimmed milk in TBS-tween (0.1%) (anti-*Trichomonas* IscS, 1:1000; anti-*Giardia* IscU, 1:500; anti-*Trypanosoma* Frataxin 1:300; anti-*Erwinia* SufC, 1:1000) and applied to the membrane overnight at 4 °C. Membranes were washed as before and incubated with the secondary antibody diluted in 1% skimmed milk in TBS-tween (0.1%). Membranes were

washed as before, incubated with ECL reagent (GE Healthcare) and fluorescence was monitored by autoradiography.

Immunolocalization

Blastocystis cultures were centrifuged at 800 x g for 10 min at 4 °C and placed within an anaerobic chamber. Cells were resuspended in 1 x PBS and 200 µL/well was transferred to pretreated poly-l-lysine slides (Sigma). Slides were incubated at room temperature for 2 hr within the anaerobic chamber. Cells were washed for 5 min in 1X PBS. The slides were removed from the anaerobic chamber and fixed with 3.7% formaldehyde/0.5% acetic acid for 15 min at 37 °C. Cells were washed for 5 min in PBS/0.5% tween-20 and then permeabilized with ice-cold acetone for 5 min. Washes were performed 3 times for 5 min in PBS/0.5% tween-20 and slides were incubated in 1 x PBS containing 200 nM of Mitotracker (Invitrogen) resuspended in DMSO for 20 min anaerobically in the dark. The exposure to light was limited from this point on. The slides were washed 3 times in PBS/0.5% tween-20. The fixed cells were then blocked for 1 hr with 5% skimmed milk in PBS/0.5% tween-20. They were washed for 30 min with 0.5% milk in PBS/0.5% tween-20 and incubated with primary antibody in 1% milk in PBS/0.5% tween-20 overnight at 4 °C. The anti-*Trichomonas* IscS, (dilution 1:200), the anti-*Giardia* IscU (1:100) the anti-*Trypanosoma* Frataxin (1:50) and the anti-*Erwinia* SufC (1:500) were used on the fixed cells. Fixed cells were then washed 3 times or 10 min with 0.5% milk in 1 x PBS solution and incubated with secondary antibody (1:1000 dilution) in 1% milk/1 x PBS solution for 1 hr. Cells were then washed 3 times for 10 min in 1 x PBS. Slides were incubated at room temperature for 5 min with DNA staining

DRAQ5 (1:1000 dilution) in 1 x PBS and then washed 3 times for 10 min in 1X PBS. A drop of VECTASHIELD Mounting Medium (Vector Laboratories Inc.) was added to each well and a cover slip was placed on. The slides were viewed under confocal microscopy (Zeiss LSM 510 Meta).

Purfication of *Blastocystis* mitochondrion-related organelles and other subcellular fractions.

MROs were isolated following the procedures described previously (24, 25) with slight modifications. *Blastocystis* cells were harvested by centrifiguation at 1200 x g for 10 mins at 4 ^{o}C. Cells were resuspended in Locke's solution (pH 7.4) and centrifuged as again with the same speed and duration. Cells broken with 40 strokes in 10 ml Potter-Elvehjem tissue homogenizer at 4 °C in isotonic buffer (200 mM sucrose (pH 7.2), 30 mM phosphate, 15 mM β-mercaptoethanol, 30 mM NaCl, 0.6 mM $CaCl_2$, 0.6 mM KCl). Broken cells were then diluted with isotonic buffer (buffer had been degassed and air replaced with nitrogen) and then centrifuged at 500 x g for 10 min using Sorvall RC-2B to remove unbroken cells. The supernatant was collected and centrifuged at 5000 x g for 10 min to pellet the Large Granular Fraction; LGF (where MROs are found – see 24,25) and again at 25000 x g for 20 min to obtain a pellet of the Small Granular Fraction; SGF. A two-steps density gradients were prepared from 15 and 65% (w/w) sucrose; large and small granular fractions were layered on top and centrifuged in 6 x 12 swing-out rotor (SW 41 Ti) at 4 °C for 1 hour at 46,000 x g. The fractions were collected using an 1ml syringe without disturbing the gradient and were subsequently washed with isotonic buffer.

TEM specimen preparation for immunolabeling

Blastocystis NandII cultures were centrifuged at 1500 x g for 10 min at 4 °C. Samples were fixed in the anaerobic chamber with 4% paraformaldehyde/0.5% glutaraldehyde in 0.1 M sodium cacodylate buffer for 30 min. Samples were rinsed 3 times for 10 min with 0.1 M sodium cacodylate buffer. Samples were dehydrated with a graduated series of ethanol: 50% ethanol for 10 min, 70% ethanol 2 times for 10 min, 95% ethanol 2 times for 10 min, 100% ethanol 2 times for 10 min and dried 100% ethanol for 10 min. Samples were then infiltrated with LR white resin: 3 parts dried 100% ethanol and 1 part resin for 3 hr, 1 part dried 100% ethanol and 3 parts resin overnight and 100% resin 2 times for 3 hr. Samples embedded in resin were placed in a 60 °C oven for 48 hr and then cut using a LKB Huxley ultramicrotome with a diamond knife and placed on 300 mesh nickel grids. Samples were viewed with a JEOL JEM 1230 transmission electron microscope to determine quality before proceeding with immunolabeling. The anti-*Erwinia* SufC antibody was recognized by secondary antibodies conjugated to 10 nm colloidal gold particles.

Complementations in *Trypanosoma* KD strains

The full-length cDNAs of the *Blastocystis* IscS, IscU and frataxin genes (1374, 456 and 456 nt respectively) were cloned into the pABPURO vector with or without the HA_3 tag at its 3' end (using primers introducing ClaI and HindIII restriction sites; **Table S2**), following the cloning strategy described previously (11). In addition, the full length *Phaeodactylum triconutum isd11*, was cloned in the *T. brucei* PCF-4 vector. Regions

encoding mitochondrial targeting peptides of the *Blastocystis* IscS, IscU and frataxin proteins, predicted with MitoProt (26) with high probabilities (>0.97), were retained in the constructs for the rescue experiments. The linearized construct was introduced into the inducible knock-downs PF *T. brucei* cells for TbIscS, TbIscU and TbFrataxin respectively as described previously (11).

Measurement of enzymatic activities. We measured activities of fumarase, aconitase and threonine dehydrogenase in the cytosolic and mitochondrial fractions obtained with digitonin fractionation. The purity of the subcellular fractions were monitored by compartment-specific antibodies against MRP2 and enolase in western blot analysis. To determine the activities of fumarase and aconitase we monitored the production of fumarate and cis-aconitate respectively by measuring increasing absorbance at 240 nm. The activity of threonine dehydrogenase was measured by recording changing absorbance at 340 nm as an indicator of the rate of NAD^+ reduction as described elsewhere (27). The activity of succinate dehydrogenase was measured in crude mitochondrial membrane extract as described previously (28).

Phylogenetics

For each protein, query sequences were used to mine the various genomic and EST sequence databases using BLAST searches against all available eukaryotic genomes and representatives from the bacterial and archaeal groups. The collected sequences were aligned using MUSCLE (29) and trimmed manually. To test if the aligned SufC and SufB sequences were phylogenetically congruent we used Concaterpillar 1.4 (30).

Phylogenetic trees were estimated from alignments using RAxML7.0.4 (31) using the LG+Gamma+F model of amino acid substitution. Bayesian phylogenetic analysis was also carried out using MrBayes (32) and Phylobayes (33) using the same models. Topology testing was performed using Consel (6) for the approximately unbiased (AU) test and RaxML7.0.4 (31) for the Shimodaira-Hasegawa (SH) and expected likelihood weights (ELW) tests.

Expression and purification of SufS, SufE and SufBC$_2$D from *E. coli*. Plasmid pGSO164 containing the entire *suf* operon from *E. coli* was used to express the SufBC$_2$D complex (34). Plasmids pET-Shis, pET-Ehis encoding the His-tagged SufS and SufE from *E. coli* were obtained as previously described (35-37). Plasmid pG5783 encoding aconitase B was kindly provided by J.R. Guest (Norwich, UK). (His)$_6$-SufE and SufABCDSE from *E. coli* were produced in *E. coli* TOP10 cells (Invitrogen), (His)6-SufS as well as AcnB were produced in *E. coli* BL21(DE3) plysS cells (Invitrogen) as described previously (3). Cells were grown in LB medium in the presence of 100µg/ml ampicillin or 30µg/ml chloramphenicol at 37°C to an A600 = 0.5 before induction with 0.2% L-arabinose (w/v) or 0.5 – 1 mM IPTG. Cells were grown at 37°C for a further 5 hours. Purification of SufS and SufE was then performed as described in (38). For SufBC$_2$D cell-lysis and purification methods see (3, 35).

Characterization of *Blastocystis* SufCB

Cloning: The full-length cDNA of the *Blastocystis SufCB* gene (2100 nt) was cloned into the pET16b vector (Novagen) using primers BhSufC_Nde_F and BhSufC_Nde_R (**Table S2**), which introduce NdeI and XhoI restriction sites respectively.

Expression. To express *Bh*-SufCB, pET16b-sufCB was transformed into C43(DE3) competent cells (39) that were grown on LB plates with 100 μg/ml ampicillin. A single colony was inoculated into 100 ml LB (100 μg/ml ampicillin), and the culture was grown at 37°C overnight, transferred into 10 L of LB (containing 100 μg/ml ampicillin), and grown with shaking at 120 x g at 37°C. When the absorbance at 600nm reached 0.5, protein expression was performed by adding IPTG 0.5 mM and the culture was incubated at 25°C overnight. Cells were then harvested by centrifugation at 3200 x g at 4°C for 15 min. The cells were suspended in 100 mL of 50 mM Tris-HCl pH 7.5, harvested at 3200 x g for 20 min at 4°C and stored at -80°C.

Purification of SufCB from Blastocystis. To purify *Bh*-SufCB, the cells were thawed and resuspended in 0.1 M Tris-HCl pH 8, 50 mM NaCl, 1 mM PMSF, 5 mM β-mercaptoethanol. Cell walls were broken by sonication for 15 min. (15 times, 20 sec at 30% amplitude). The insoluble debris, including the inclusion bodies made predominantly of *Bh*-SufCB, were centrifuged at 20000 x g 60 min at 4°C. The combined pellets were suspended in 120 mL of 0.1 M Tris-HCl pH 7.5, 100 mM dithiothreitol (DTT) and 6M guanidine-HCl (or urea) and stirred for 4 hours at RT. The suspension was then pelleted by centrifugation at 6400 x g for 20 min. at RT. DTT was removed by dialysis at 4°C against 0.1 M Tris-HCl pH 7.5, 6M guanidine buffer. The clear red-brown solution was then loaded onto an 5 mL NiNTA column (Stratagene) equilibrated with 0.1 M Tris-HCl pH 7.5, 6M guanidine-HCl buffer. After an extensive washing using first, the

same buffer, and second, the same buffer containing 20 mM imidazole, the protein was eluted with 0.1 M Tris-HCl pH 6, 50 mM NaCl, 400 mM imidazole. Complete refolding was accomplished using a desalting NAP-25 column (GE-Healthcare) equilibrated with 0.1 M Tris-HCl pH 6, 50 mM NaCl buffer. Protein fractions were concentrated on a Millipore Amicon device and the pools were loaded onto a gel-filtration chromatography column (Sdx-200 from Pharmacia-Amersham) equilibrated with 0.1 M Tris-HCl pH 6, 50 mM NaCl buffer. Fractions containing *Bh*-SufCB were concentrated and stored at -80°C before use.

Cysteine desulfurase activity. Assays were performed in 25 mM Tris, pH 7.5, 100 mM NaCl, 100 µM DTT in a final volume of 100 µl. Final protein concentrations were 500 nM of *E. coli* SufS and 1.5 µM of *E. coli* SufE and *E. coli* $SufBC_2D$ or *Bh*-SufCB. Reactions were initiated by addition of 100 µM L-cysteine (final concentration) and were allowed to proceed for 20 min at 27°C. Reactions were stopped by heating the mixtures at 99°C for 10 min. Denatured proteins were removed by centrifugation and the supernatant was analyzed for its alanine content using alanine dehydrogenase (40). The absorbance of NADH at 340 nm (ε340nm = 6.2 mM-1cm-1) was used to determine the alanine content of the cysteine desulfurase activity assay mixtures.

Iron-sulfur cluster chemical reconstitution. Purified *Bh*-SufCB (135 µM) was incubated with a 6-fold molar excess (810 µM) of $Fe(NH_4)_2(SO_4)_2$ and Na_2S in the presence of 5 mM DTT at 18 °C under anaerobic conditions. After 4 h incubation, the mixture was desalted using a NAP-25 column (GE Healthcare). UV-visible spectrum of reconstituted *Bh*-SufBC was recorded on a Cary 1 Bio (Varian) spectrophotometer. The iron and sulfur content of the complex was determined as previously described (41, 42).

Reconstitution of Bh-SufCB with flavin. *Bh*-SufBC protein was first desalted in 50 mM Tris-HCl pH 7.5 under anaerobic conditions and then incubated in the same buffer under anaerobic conditions with a 5-fold molar excess of FAD. Photo-induced reduction of the flavin was achieved by irradiation with a commercial slide projector placed at a distance of 3 cm in the presence of 5-10 mM DTT (43). The resulting solution was desalted with a NAP-25 (GE-Healthcare) column to remove unbound flavin. After aerobic heat denaturation of the protein, the concentration of protein-bound $FADH_2$ was calculated from the absorbance of free oxidized FAD at 450 nm (ε:11. 300 $mM^{-1}.cm^{-1}$).

Iron-sulfur cluster transfer reaction. All Fe/S transfer-experiments were performed anaerobically at 18 °C. Aconitase B in its *apo*-form (0.2 nmol) was first treated with 5 mM DTT for 30 min, before desalting the protein solution with a MicroBiospin column (Biorad). The resulting protein (0.2 nmol) was then incubated in 50 mM Tris-HCl pH 7.6 with either a 1.5-fold molar excess of the *Bh*-SufBC-(Fe/S) (0.3 nmol) in order to provide sufficient equivalent of Fe and S to built a [4Fe-4S]/AcnB or with 5 molar excess of iron and sulfide. Aconitase activity was assayed after 10 min. incubation in 100 µl by monitoring the formation of NADPH via the increase of absorbance at 340 nm as described by Gardner and Fridovitch (44).

ATPase assay. The ATPase activity was tested by measuring the amounts of P_i released by ATP hydrolysis with the use of Malachite green reagent (45). The assay was performed for 5 min using 10 µM SufBC from *Blastocystis* in 25 mM Tris-HCl pH 7.5 buffer in the presence of 5 mM $MgCl_2$ and ATP (0-2 mM) at 30°C. The reaction was stopped by addition of 50 mM EDTA.

Determination of protein concentration. Protein concentrations were measured by the Bradford method using bovine serum albumin as a standard.

Complementation experiments with *Bh*-SufCB

In *E. coli* the SUF system is required to cope with iron starvation, we then tested whether the *Blastocystis* SufCB protein can compensate the lack of the SufB or the SufC proteins under iron starvation conditions. We thus performed an heterologous complementation assay using Δ*sufB* or Δ*sufC E. coli* strains. The *Blastocystis sufCB* gene was expressed from the p*araBAD* promoter or p*trp-lac* promoters of the pBAD24 and pTrc99A plasmid derivatives, respectively. Tables I and II showed that expression of the *sufCB* gene, from pBAD24 or pTrc99A derivatives, did not allow the *sufC* mutant to grow in the presence of the iron chelator (Dipyridyl). In control, plasmids carrying a copy of the *E. coli sufC* gene, pT-Ec-sufBCD and pB-Ec-sufC, rescued growth defect of the *sufC* mutant in the presence of dipyridyl, albeit complementation using pT-Ec-sufBCD was less efficient that with the pB-Ec-sufC.

We then used the *E. coli* strain deleted of *sufB*, and showed that expression of the *Blastocystis sufCB* gene did not allow the *sufB* mutant to grow in the presence of the dipyridyl, either from pBAD or pTrc derivatives (Tables III and IV). In contrast, plasmids carrying the *E. coli sufB* gene, pB-Ec-sufB and pT-Ec-sufBCD, were able to rescue growth of the *sufB* mutant in presence of dipyridyl (250µM) (Table III and IV).

In order to test whether heterologous complementation was prevented because of the presence of the two remaining components of the SufBCD scaffold in the *sufC* and

sufB mutants, (SufB and SufD in the *sufC* mutant, and SufC and SufD in the *sufB* mutant) we constructed a strain lacking all components of the SufBCD scaffold (Δ*sufBCD*). In this strain, plasmids carrying the *sufCB* gene of *Blastocystis* did not rescue growth defect due to the presence of dipyridyl.

All together theses results suggest that the *Blastocystis* SufCB protein is not able to compensate for the lack of SufC or SufB in *E. coli* under iron deprivation conditions.

Table I

	Glu 0.2% Dipyridyl (µM)			Ara 0.2% Dipyridyl (µM)		
	0	250	320	0	250	320
Strains						
wt/pBAD24	+	+	+	+	+	+
sufC/ pBAD24	+	-	-	+	-	-
sufC/ pB-blasto-sufCB	+	-	-	+	-	-
sufC/ pB-Ec-sufC	+	-	-	+	+	+

Strains were streaked onto LB plate containing glucose (0.2%) or arabinose (0.2%) supplemented or not with dipyridyl at the indicated concentration. Growth was scored after an overnight incubation at 37°C (+ and - indicates growth and absence of growth, respectively).

Table II

	No IPTG Dipyridyl (µM)			IPTG 1mM Dipyridyl (µM)		
	0	250	320	0	250	320
Strains						
Wt/pTrc99A	+	+	+	+	+	+
sufC/ pTrc99A	+	-	-	+	-	-
sufC/ pT-blasto-sufCB	+	-	-	+	-	-
sufC/ pT-Ec-sufBCD	+	+ *	+ *	+	+ *	-

Strains were streaked onto LB plate supplemented or not with IPTG and dipyridyl at the indicated concentration. Growth was scored after an overnight incubation at 37°C (+ and - indicates growth and absence of growth, respectively. Asterisk indicates that the strain formed small colonies).

Table III

	Glu 0.2% Dipyridyl (µM)	Ara 0.2% Dipyridyl (µM)

	0	250	320	0	250	320
Strains						
Wt/pBAD24	+	+	+	+	+	+
D*sufB*/ pBAD24	+	-	-	+	-	-
D*sufB*/ pB-blasto-sufCB	+	-	-	+	-	-
D*sufB*/ pB-EC-sufB	+	+*	-	+	+*	-

Strains were streaked onto LB plate containing glucose (0.2%) or arabinose (0.2%) supplemented or not with dipyridyl at the indicated concentration. Growth was scored after an overnight incubation at 37°C (+ and - indicates growth and absence of growth, respectively. Asterisk indicates that the strain formed small colonies)

Table IV

	No IPTG			IPTG 1mM		
	Dipyridyl (µM)			Dipyridyl (µM)		
	0	250	320	0	250	320
Wt/pTrc99A	+	+	+	+	+	+
D*sufB*/ pTrc99A	+	-	-	+	-	-
D*sufB*/ pT-blasto-sufCB	+	-	-	+	-	-
D*sufB*/ pT-Ec-sufBCD	+	+*	-	+	+*	-

Strains were streaked onto LB plate supplemented or not with IPTG and dipyridyl at the indicated concentration. Growth was scored after an overnight incubation at 37°C (+ and - indicates growth and absence of growth, respectively. Asterisk indicates that the strain formed small colonies).

Fe/S cluster maturation *in vivo*.

Media and growth conditions

The rich medium used in this work was LB broth (46). Arabinose (0.2%), casaminoacids (0,2%), amino acids (0,005%), thiamine (50 µg/ml), nicotinic acid (12,5 µg/ml) and mevalonate (1 mM) were added when required. Solid media contained 1.5% agar. Antibiotics were used at the following concentrations: chloramphenicol (Cm) 25 µg/ml, kanamycin (Km) 25 µg/ml, and ampicillin (Amp) 50 µg/ml.

Strains construction

The *E. coli* strains DV1331 (Δ*lacZ* P_{hmpA}::*lacZ sufCD iscUA::cat* MVA+) and DV1185 (Δ*lacZ* P_{iscR}::*lacZ sufCD iscUA::cat* MVA+) are *E. coli* K-12 derivatives. The transcriptional P_{hmpA}::*lacZ* and P_{iscR}::*lacZ* fusions were constructed as described in Vinella *et al* (in preparation) (47) and the Δ*iscUA*::*cat*, and Δ*sufCD* mutations were constructed as previously described (48, 49). The donor of the MVA+ Kan^R cassette was

strain DV1093 (48). All mutations were introduced into strains by P1 *vir* transduction (46), selecting for the appropriate antibiotic resistance. The antibiotic resistance cassettes were eliminated when needed using plasmid pCP20 as described (48). The construction of all the conditional-lethal mevalonate-dependent strains was carried out in anaerobiosis with mevalonate in the plates to limit the occurrence of suppressor mutations (48).

Table V
Bacterial strains and plasmids

Strain	Relevant genotype	Origin or construction
MG1655	Parental strain	Laboratory collection
DV206	MG1655 Δ*lacZ*	(50)
DV1093	MG1655 MVA+	(48)
DV597	MG1655 Δ*iscUA*::*cat*	(48)
DV813	Δ*lacZ* Δ*sufCD*::*kan*	DV206 + P1/JW1672 (49), selection LB Km. This study
DV828	Δ*lacZ* Δ*sufCD*	DV813 cured with pCP20. This study
DV1304	Δ*lacZ* P_{hmpA}::*lacZ* Δ*sufCD*	Lysogen of DV828. This study
DV1310	Δ*lacZ* P_{hmpA}::*lacZ* Δ*sufCD MVA+*	DV1304 + P1/DV1093. This study
DV1331	Δ*lacZ* P_{hmpA}::*lacZ* Δ*sufCD* MVA+ Δ*iscUA*::*cat*	DV1310 + P1/DV597, selection en LB Cm mev ara. This study
DV1185	Δ*lacZ* P*iscR*::*lacZ* Δ*iscUA* MVA+ Δ*sufCD*::kan Tn10	(51)
Plasmid		
pBAD24	Cloning vector	(52)
pBAB-*sufCB*	pBAD24 derivative carrying the *Blastocystis sufCB* gene	This study
pBAD-*sufABCDSE*	pBAD24 derivative carrying the *E. coli suf* operon	(53)

Quantitative RT-PCR

RNA isolation and cDNA synthesis. Total RNA was harvested from *Blastocystis* Nand II cells incubated for 1 and 10 minutes on a shaking platform (230 rpm) using Trizol reagent (Invitrogen, Burlington, ON) according to manufacturer's specifications. The quality of the resulting RNA was checked both by gel electrophoresis and by spectrophotometry. The RNA was quantified and all samples were adjusted to the same

concentration. Subsequently, RNA was treated with DNase I (Invitrogen, Burlington, ON) and TURBO^{TM} DNase (AMBION, Streetsville, ON) to minimize genomic DNA contamination. The first strand was synthesized using an oligo dT primer and Superscript II (Invitrogen, Burlington, ON). For each treatment, a no Superscript II control was included.

Quantitative RT-PCR primers. Primers were designed using the Oligo Primer Analysis software. The primers were checked for duplex formation, 3′-end stability and repeats.

GAPDH: Fwd, 5′-GAAGAAGCCCGCCAC-3′

Rev, 5′-GTCAGCAGATCGCGAGACA-3′

IscS: Fwd, 5′-GGGGATTCAAGATCACATACC-3′

Rev, 5′-CGTTGTTGACGCCCATC-3′

SufC: Fwd, 5′-CACCATCATCATCACGCAC-3′

Rev, 5′-GAGACGTTGCGGAAATAGTTG-3′

Hsp70: Fwd, 5′-CATTACTGTGCCCGCCTACT

Rev, 5′-ACGCCTCCGCTGATCTC

Hydrogenase: Fwd, 5′-CGAGATCCTGCCGAACC-3′

Rev, 5′-ATCAGCGACACCACGTAGA-3′

RLi: Fwd, 5′-CAAGCTGAAGCCCAATCTC-3′

Rev, 5′-CCACCAGGTCGTCCATC

Quantitative PCR analysis. The analysis was performed in triplicate for each treatment in a Mastercycler® ep realplex (Eppendorf AG, Hamburg) using the DNA-intercalating

fluorescent dye SYBR Green (Invitrogen, Burlington, ON). The PCR profile included a 180s initial round of denaturation at 94.0°C, followed by 40 cycles of 20s at 94.0°C, 20s at 57.0°C and 25s at 72.0°C. Data for the analysis of the mRNA transcript expression was collected during the linear phase of amplification.

Supplementary Fig legends:

Fig S1

An alignment of *Blastocystis sufCB* sequences from genomic and complementary DNA. The alignment demonstrates the presence of 10 canonical spliceosomal introns (GT - AG splicing boundaries) in the genomic sequence, showing that the gene is not from a bacterial contaminant.

Fig S2

The distribution of the SUF system amongst microbial genomes (modified from Tokumoto et al., 2004 (1)). Since the *sufBC*-like genes are found in all species encoding this system, it has been speculated that these genes were components of the primitive system, which was further evolved through the recruitment of other components such as SufA, SufE and SufS (e.g. *E. coli* Suf system). We have identified a gene in *Blastocystis* genome/transcriptome corresponding to the SufCB operon in bacteria. The SufCB operon encodes two out of the six proteins of the SUF system (e.g *E. coli*) and is part of the Suf system found in extremophiles.

Fig S3

The phylogeny of SufB. The SufB tree was estimated by maximum likelihood (RAxML) and Bayesian analysis (MrBayes) from selected sequences from within the Bacteria, Archaea and Eukaryotes. The tree was generated from 318 aligned amino acids (111 taxa) using the LG model with gamma correction. *Blastocystis* SufB branches within an extremophile clade, and, with strong bootstrap support (97) and posterior probability (1.0) as a sister group to the methanoarchaea. Only bipartitions that received >65% ML bootstrap support are labelled with support values.

Fig S4

The phylogeny of SufC. The SufC tree was estimated by maximum likelihood (RAxML) and Bayesian analysis (MrBayes) from available sequences from Bacteria, Archaea and Eukaryotes. The tree was generated from 214 aligned amino acids (111 taxa) using the LG model with gamma correction. *Blastocystis* SufC clusters within extremophiles with a weak bootstrap support and posterior probability. Only bipartitions that received >65% ML bootstrap support are labelled with support values.

Fig S5

Complete phylogeny of a SufBC concatenated tree estimated by maximum likelihood (RAxML) and Bayesian analysis from available sequences from Bacteria, Archaea and Eukaryotes. The tree was generated from 532 aligned amino acids (111 taxa) using the LG+Gamma model. *Blastocystis* SufCB clusters within extremophiles, and with a strong

bootstrap support (95) and posterior probability (1.0/0.99) as a sister group to the Methanobacteriales. Since the *Blastocystis* homolog does not cluster with other stramenopiles, these data strongly suggest a Lateral Gene Transfer (LGT) event between the two taxa. Support values for branches are shown above them in the following order: maximum likelihood bootstrap support (LG+G+F model, RAxML)/posterior probability (LG+G+F model, MrBayes)/posterior probability (C20 model, PHYLOBAYES). Only bipartitions that received >65% ML bootstrap support are labelled with support values.

Fig S6

Bh-SufCB* is involved in the Fe/S clusters maturation in *E. coli. *E. coli* strains harbouring the P_{hmpA}::*lacZ* fusion (DV1331) (a) or the P_{iscR}::*lacZ* fusion (DV1185) (b) and carrying the indicated pBAD24 derivative plasmids were grown in LB supplemented with mevalonate, arabinose, thiamine, and nicotinic acid, at 37°C. ß-galactosidase assays were carried out as described (46) when culture cells reached an OD600 nm of 0.4-0.6 after dilution of fresh overnight cultures. Activity are expressed in percentage using as 100% the activity obtained in strains carrying the empty vector (pBAD24), 2270+/-410 and 850+/-50 miller units for the P_{hmpA}::*lacZ* fusion and P_{iscR}::*lacZ* fusion, respectively.

Fig S7

Far UV (A) and near UV (B) spectra of *Bh*-SufCB-Fe/S. For all spectra, proteins were diluted in 50 mM Tris-HCl pH 8 at a final concentration of 0.65 µM. Spectra were recorded on a J-815 spectropolarimeter (Jasco, Tokyo, Japan) at 22°C with constant N_2 flushing. The scans were recorded using a bandwidth of 2 nm and an integration time of 1

s at a scan of 0.5 nm/s. Each spectrum is the average of 10 scans corrected for the blank and not smoothed.

Fig S8

Spectroscopic characterization of *Bh*-SufCB-Fe/S. UV-visible spectrum of anaerobically reconstituted *Bh*-SufCB (20 µM) containing 4.2 mol of iron and 4.5 mol of sulfur / mol of *Bh*-SufCB dimer. Inset : EPR spectrum of anaerobically reconstituted *Bh*-SufCB (100 µM) reduced with 2 mM dithionite. T=5 K ; P=0.1 mW ; gain=$2x10^5$; amplitude modulation=10 mT.

Fig S9

A SufB alignment. The conservation of functionally important residues in the *Blastocystis* SufB sequence in aligned with homologs from other eukaryotic, bacterial and archaeal genomes. Green highlighted residues correspond to conserved residues among Methanomicrobiales, whereas blue highlights correspond to conserved residues among all homologs. Grey highlight and bold residues correspond to FAD binding motifs in SufB from *E. coli* (3), which are absent in Methanomicrobiales and in *Blastocystis*. Cysteine residues are colored in red.

Fig S10

Western blot analyses of the expression of *Blastocystis* SufCB, IscS, IscU and frataxin. a. (1) Identification of the *Blastocystis* SufCB recombinant protein using an antibody to the His-tag. The antibody recognizes a band at an apparent relative molecular

mass (M_r) of about ~78 kDa, which is not present in *E. coli* protein extract controls. **(2)** A western blot using heterologous antiserum to *Erwinia chrysanthemi* SufC (7, 10) *Blastocystis* recombinant protein (the lane labelling is the same as in **1)**. The antiserum shows specific detection of *Blastocystis* recombinant SufCB protein in *E. coli* cells expressing the protein. The protein has an apparent relative molecular mass (M_r) of about 78 kDa, similar to the band identified using the His-tag antibody. **(3)** Western blot using heterologous anti-*Erwinia chrysanthemi* SufC (7, 10) antisera to *Blastocystis* total cell lysates shows specific detection of *Blastocystis* SufCB with an apparent relative molecular mass of 77 kDa. **b.** Western blot using heterologous anti-*Trichomonas* IscS (9) antisera to *Blastocystis* total cell lysates shows specific detection of *Blastocystis* IscS with an apparent relative molecular mass of 50.8 kDa. **c.** Western blot using heterologous anti-*Giardia* IscU (10) antisera to *Blastocystis* total cell lysates shows specific detection of *Blastocystis* IscU with an apparent relative molecular mass of 16.3 kDa. **d**. Western blot using heterologous anti-*Trypanosoma* frataxin (11) antisera to *Blastocystis* total cell lysates shows specific detection of *Blastocystis* frataxin with an apparent relative molecular mass of 16.9 kDa. **e.** Western blots demonstrating the cellular localization of the *Blastocystis* SufCB. The heterologous anti-*Erwinia chrysanthemi* SufC antisera shows specific detection of *Blastocystis* SufCB with an apparent relative molecular mass of 77 kDa in the cytosolic fraction, but absent in the Large Granule Fraction (LGF), that is consistent with the absence of this protein in the MROs.

Fig S11

Two additional images demonstrating the cytosolic localization of SufCB in *Blastocystis* cells by transmission electron microscopy. Insets are enlargements of specific regions of the cell, focusing in the localization of SufCB within the different compartments of the cell but also the distribution of the protein within the cytosol.

Fig S12

Immunolocalization of IscU and Frataxin. a. Rabbit anti-*Giardia* IscU antibodies (1:100) detect *Blastocystis* IscU. **e**. Rabbit anti-*Trypanosoma* frataxin antibodies (1:50) detect the *Blastocystis* frataxin. **b,f.** Mitotracker red labels discrete structures corresponding to the mitochondrion-related organelles (MRO) of *Blastocystis*. **c,g.** Co-localization of mitotracker red with the above ISC proteins. **d,h.** Differential interference contrast (DIC) images of the cells used for immunofluorescence. Scale bar: 10 μm.

Fig S13

Identification of candidate functionally important residues in *Blastocystis* frataxin sequence. Frataxin contains two highly conserved surface exposed regions: a semi-hydrophobic patch on the β sheet surface that was proposed to take part in intermolecular interactions, and a negatively charged region comprising residues in the helix α1 and the beta sheet β1 which represents the iron-binding region (54). Putative residues involved in iron binding based on NMR spectroscopy and mutant studies are highlighted in blue (54-56). Residues of *E. coli* with the highest affinity for Fe^{2+} (54, 55) are highlighted in **bold**. Candidate iron-binding amino acids from *Blastocystis* are highlighted in red. Common iron binding ligands in proteins involve Asp, Glu, His and Cys residues.

Fig S14

Conservation of functionally important residues in the *Blastocystis* cysteine desulfurase (IscS). Sequence alignment of eukaryotic Nfs1 and IscS protein sequences with bacterial IscS orthologs and paralogous NifS sequences. Residues involved in binding pyridoxal phosphate (PLP) (57, 58) are highlighted in yellow. Residues involved in substrate binding are highlighted in green. The substrate cysteine is anchored by a salt bridge to Arg393 and Asn186. Asn67 forms a hydrogen bond to the substrate (58). The PLP-binding Lys240 residue (57-59) is highlighted in turquoise. The Cys367 residue, essential for cysteine desulfurase (59) is highlighted in pink. The conserved His138 residue, highlighted in red, is involved in several protonation and deprotonation steps (57, 58). The nuclear targeting signal sequence RRRPR that is required for survival of yeast cells (60) is highlighted in dark green. The Cys residue conserved (61) in all eukaryotic Nfs1 and in *Rickettsia prowazekii* IscS is highlighted in grey. Key to organism names: Blasto: *Blastocystis* sp. NandII; Ho_sap, *Homo sapiens*; Sa_cer, *Saccharomyces cerevisiae*; Tr_vag, *Trichomonas vaginalis*; Cr_par, *Cryptosporidium parvum*; Ri_pro, *Rickettsia prowazekii*; Es_col, *Escherichia coli*; Az_vin, *Azotobacter vinelandii*.

Fig S15

Conservation of functionally important residues in *Blastocystis* scaffold protein (IscU) sequence. Sequence alignment of Isu protein sequences against orthologous bacterial IscU and paralogous NifU sequences. The conserved tyrosine residue found in virtually all Isu/IscU/NifU proteins is highlighted in green. Conserved cysteine residues

(BlastIscU 49, 73 and 116) that form the critical iron-binding site are highlighted in grey (62, 63). Residues in Isu/IscU family members that are responsible for the functional interaction (64) with mtHsp70 are highlighted in blue. This motif is not present in NifU. The conserved aspartate-51 residue that is thought to play a role of the release of transient Fe/S from NifU (65) is highlighted in yellow. Key to organism names: Blasto: *Blastocystis* sp. NandII; Ho_sap, *Homo sapiens*; Sa_cer, *Saccharomyces cerevisiae*; Tr_vag, *Trichomonas vaginalis*; Cr_par, *Cryptosporidium parvum*; Ri_pro, *Rickettsia prowazekii*; Es_col, *Escherichia coli*; Az_vin, *Azotobacter vinelandii*.

Fig S16

Functional characterization of *Blastocystis* frataxin. a. Effect of growth on the non-induced (black empty circles) and RNAi-induced Tb-frataxin knock-down transfected with constitutively expressed *Blastocystis* frataxin (grey full circles). **b.** Effect of depletion of *Tb*-frataxin by RNAi on the growth of the procyclic *Trypanosoma* cells (non-induced: grey empty squares; induced: black triangles). **c**. Effect of the depletion of *Tb*-frataxin by RNAi on the growth of the procyclic *Trypanosoma* cells transfected with an empty pABPURO vector (non-induced: grey empty triangles; induced: black triangles). **d,e**. Activities of aconitase and fumarase respectively in total *Tb*-frataxin cell lysates after 5 days of RNAi induction, respectively **f.** Activities of threonine dehydrogenase, a non-Fe/S protein, was not affected by the ablation of *Tb*-frataxin. Hatched bars: WT: 29-13 wild type strain of *T. brucei*; empty bars: non-induced RNAi knock-down cells; grey bars: RNAi-induced knock-down cells. **g.** Western blot demonstrating the cellular localization of the *Blastocystis* HA-tagged frataxin in *T.*

brucei. Enolase and mitochondrial RNA binding protein 2 (MRP2) served as cytosolic and mitochondrial markers, respectively. KD: knock-down strain.

Fig S17

Functional characterization of *Blastocystis* IscS. a. Effect of growth on the non-induced (black empty squares), on RNAi-induced Tb-IscS knock-downs transfected with constitutively expressed *Blastocystis* IscS (grey full squares), on the non-induced (black empty triangles) and RNAi-induced Tb-IscS knock-downs transfected with constitutively co-expressed *Blastocystis* IscS and *Phaeodactylum tricornutum* (Ptr)-Isd11 (grey full triangles). **b.** The effect of depletion of *Tb*-IscS by RNAi knockdown on the growth of the procyclic *Trypanosoma* cells (non-induced: black empty triangles; induced: grey triangles). **b.** The effect on growth of the *Tb*-IscS RNAi knockdown cells transfected with *Blastocystis* IscS and an empty vector pFC4 (non-induced: black empty triangles; induced: grey triangles). **d.** Activities of aconitase in total *Tb*-IscS RNAi knockdown cell lysates after 5 days of RNAi induction. Hatched bars: WT: 29-13 wild type strain of *T. brucei*; empty bars: non-induced RNAi knockdown cells; grey bars: RNAi-induced knock-down cells. **e.** Activities of succinate dehydrogenase in total *Tb*-IscS RNAi knockdown cell lysates after 5 days of RNAi induction. Hatched bars: WT: 29-13 wild type strain of *T. brucei*; empty bars: non-induced RNAi knockdown cells; grey bars: RNAi-induced knock-down cells. **f.** The activity of threonine dehydrogenase, a non-Fe/S protein, was not affected by RNAi knockdown of *Tb*-frataxin. Enolase and mitochondrial RNA binding protein 2 (MRP2) served as cytosolic and mitochondrial markers,

respectively **e.** Western blot analysis demonstrating the localization of *Blastocystis* IscS both in the mitochondrion and cytosol of *Trypanosoma*. KD: knock-down strain.

Fig S18

Alignment of a taxonomically diverse representation of putative Isd11 proteins. Residues with at least 50% conservation are shaded in purple. The LYR/K residue block (Pfam PF05347) conserved in the Isd11 and the B14 and B22 components of mitochondrial complex I are illustrated. Note that *Trypanosoma* (and Excavates in general) posses a tyrosine deletion at the LYR/K block, a residue that is mostly conserved among all representatives.

Fig S19

Schematic model for Fe/S cluster assembly systems of *Blastocystis*. The *Blastocystis* MRO has maintained the basic components for the assembly of Fe/S clusters in the organelle (proteins in grey colour are currently not found in the *Blastocystis* genomes). An unknown component from this reaction is then exported to the cytosol of the parasite, whereas components of the CIA machinery are involved in the support of the cytosolic and nuclear apo-proteins. Upon exposure to oxygen, the SUF machinery takes over to potentially support the inactive Fe/S Holo-proteins.

Fig S20

Effects of atmospheric oxygen exposure on gene expression of selected genes relative to a GAPDH control measured by quantitative reverse-transcriptase PCR. Cells were

incubated anaerobically (black), in atmospheric oxygen for 1 minute (green) or for 10 minutes (red). The genes assayed were *Blastocystis sufCB*, cysteine desulfurase (*iscS*), [FeFe]-hydrogenase (*hyd*), RNAase L- inhibitor 1 (*rlil1*) and heat shock protein 70 (*hsp70*).

Fig S21

A SufC alignment. The conservation of functionally important residues in *Blastocystis* SufC sequence aligned with homologs from other eukaryotic, bacterial and archaeal genomes. Light blue color highlights residues that are reconstitute the Walker A and Walker B whereas yellow color highlights the H-motif. W-loop, D-loop and ABC signature are highlighted in grey. Cysteines in yellow color and highlighted in green color demonstrate the CX_nCX_2C motif, which is present in several Methanomicrobiales and in *Blastocystis* and it is potentially a domain for binding iron.

Fig S22

Conservation of functionally important residues in *Blastocystis* Nbp35 sequence (important protein that involves in the CIA machinery). Sequence alignment of Nbp35 protein sequences against homologs from other eukaryotic organisms. Green colour demonstrates the Walker A and Walker B motifs. Cysteines colored in red are the characteristic residues for the Nbp35 protein (66). Other cysteine residues are colored in blue. Yellow color highlights residues that are conserved among all eukaryotes.

Supplementary References:

1. Tokumoto U, Kitamura S, Fukuyama K, & Takahashi Y (2004) Interchangeability and distinct properties of bacterial Fe-S cluster assembly systems: functional replacement of the isc and suf operons in *Escherichia coli* with the nifSU-like operon from Helicobacter pylori. *J Biochem* 136(2):199-209 .
2. Krogh A, Larsson B, von Heijne G, & Sonnhammer EL (2001) Predicting transmembrane protein topology with a hidden Markov model: application to complete genomes. *J Mol Biol* 305(3):567-580.
3. Wollers S*, et al.* (2010) Iron-sulfur (Fe-S) cluster assembly: the SufBCD complex is a new type of Fe-S scaffold with a flavin redox cofactor. *J Biol Chem* 285(30):23331-23341 .
4. Lill R (2009) Function and biogenesis of iron-sulphur proteins. *Nature* 460(7257):831-838 .
5. Janouskovec J, Horak A, Obornik M, Lukes J, & Keeling PJ (2010) A common red algal origin of the apicomplexan, dinoflagellate, and heterokont plastids. *Proc Natl Acad Sci U S A* 107(24):10949-10954 .
6. Shimodaira H & Hasegawa M (2001) CONSEL: for assessing the confidence of phylogenetic tree selection. *Bioinformatics* 17(12):1246-1247 .
7. Nachin L, Loiseau L, Expert D, & Barras F (2003) SufC: an unorthodox cytoplasmic ABC/ATPase required for [Fe-S] biogenesis under oxidative stress. *EMBO J* 22(3):427-437 .
8. Stechmann A*, et al.* (2008) Organelles in *Blastocystis* that blur the distinction between mitochondria and hydrogenosomes. *Curr Biol* 18(8):580-585 .
9. Sutak R*, et al.* (2004) Mitochondrial-type assembly of FeS centers in the hydrogenosomes of the amitochondriate eukaryote *Trichomonas vaginalis*. *Proc Natl Acad Sci U S A* 101(28):10368-10373.
10. Tovar J*, et al.* (2003) Mitochondrial remnant organelles of *Giardia* function in iron-sulphur protein maturation. *Nature* 426(6963):172-176.
11. Long S*, et al.* (2008) Ancestral roles of eukaryotic frataxin: mitochondrial frataxin function and heterologous expression of hydrogenosomal *Trichomonas* homologues in trypanosomes. *Mol Microbiol* 69(1):94-109 .
12. Zierdt CH, Donnolley CT, Muller J, & Constantopoulos G (1988) Biochemical and ultrastructural study of *Blastocystis hominis*. *J Clin Microbiol* 26(5):965-970 .
13. Gaston D, Tsaousis AD, & Roger AJ (2009) Predicting proteomes of mitochondria and related organelles from genomic and expressed sequence tag data. *Methods Enzymol* 457:21-47 .
14. Altschul SF, Gish W, Miller W, Myers EW, & Lipman DJ (1990) Basic local search tool. *J. Mol. Biol.* 215:403-410.
15. Gish W & States DJ (1993) Identification of protein coding regions by database similarity search. *Nature Genetics* 3:266-272.

16. Thompson JD, Gibson TJ, Plewniak F, Jeanmougin F, & Higgins DG (1997) The CLUSTAL_X windows interface: flexible strategies for multiple sequence alignment aided by quality analysis tools. *Nucleic Acids Res* 25(24):4876-4882.
17. McGuffin LJ, Bryson K, & Jones DT (2000) The PSIPRED protein structure prediction server. *Bioinformatics* 16(4):404-405.
18. Tusnady GE & Simon I (2001) The HMMTOP transmembrane topology prediction server. *Bioinformatics* 17(9):849-850.
19. Sonnhammer EL, von Heijne G, & Krogh A (1998) A hidden Markov model for predicting transmembrane helices in protein sequences. *Proc Int Conf Intell Syst Mol Biol* 6:175-182.
20. Guda C, Fahy E, & Subramaniam S (2004) MITOPRED: a genome-scale method for prediction of nucleus-encoded mitochondrial proteins. *Bioinformatics* 20(11):1785-1794.
21. Claros MG & Vincens P (1996) Computational method to predict mitochondrially imported proteins and their targeting sequences. *Eur J Biochem* 241:779-786.
22. Small I, Peeters N, Legeai F, & Lurin C (2004) Predotar: A tool for rapidly screening proteomes for N-terminal targeting sequences. *Proteomics* 4(6):1581-1590.
23. Emanuelsson O, Brunak S, von Heijne G, & Nielsen H (2007) Locating proteins in the cell using TargetP, SignalP and related tools. *Nat Protoc* 2(4):953-971.
24. Nasirudeen AM & Tan KS (2004) Isolation and characterization of the mitochondrion-like organelle from *Blastocystis hominis*. *J Microbiol Methods* 58(1):101-109.
25. Lantsman Y, Tan KS, Morada M, & Yarlett N (2008) Biochemical characterization of a mitochondrial-like organelle from *Blastocystis* sp. subtype 7. *Microbiology (Reading, England)* 154(Pt 9):2757-2766.
26. Claros MG & Vincens P (1996) Computational method to predict mitochondrial imported proteins and their targeting sequences. *Eur. J. Biochem.* 241:779-786.
27. Saas J, Ziegelbauer K, von Haeseler A, Fast B, & Boshart M (2000) A developmentally regulated aconitase related to iron-regulatory protein-1 is localized in the cytoplasm and in the mitochondrion of *Trypanosoma brucei.* *J Biol Chem* 275(4):2745-2755 .
28. Horvath A*, et al.* (2005) Downregulation of the nuclear-encoded subunits of the complexes III and IV disrupts their respective complexes but not complex I in procyclic *Trypanosoma brucei*. *Mol Microbiol* 58(1):116-130 .
29. Edgar RC (2004) MUSCLE: a multiple sequence alignment method with reduced time and space complexity. *BMC Bioinformatics* 5:113.
30. Leigh JW, Susko E, Baumgartner M, & Roger AJ (2008) Testing congruence in phylogenomic analysis. *Syst Biol* 57(1):104-115 .
31. Stamatakis A (2006) RAxML-VI-HPC: maximum likelihood-based phylogenetic analyses with thousands of taxa and mixed models. *Bioinformatics* 22(21):2688-2690 .
32. Huelsenbeck JP & Ronquist F (2001) MRBAYES: Bayesian inference of phylogenetic trees. *Bioinformatics* 17(8):754-755.

33. Lartillot N, Lepage T, & Blanquart S (2009) PhyloBayes 3: a Bayesian software package for phylogenetic reconstruction and molecular dating. *Bioinformatics* 25(17):2286-2288 .
34. Outten FW, Wood MJ, Munoz FM, & Storz G (2003) The SufE protein and the SufBCD complex enhance SufS cysteine desulfurase activity as part of a sulfur transfer pathway for Fe-S cluster assembly in *Escherichia coli.* *J Biol Chem* 278(46):45713-45719 .
35. Layer G*, et al.* (2007) SufE transfers sulfur from SufS to SufB for iron-sulfur cluster assembly. *J Biol Chem* 282(18):13342-13350 .
36. Ollagnier-de-Choudens S*, et al.* (2003) Mechanistic studies of the SufS-SufE cysteine desulfurase: evidence for sulfur transfer from SufS to SufE. *FEBS Lett* 555(2):263-267 .
37. Sendra M, Ollagnier de Choudens S, Lascoux D, Sanakis Y, & Fontecave M (2007) The SUF iron-sulfur cluster biosynthetic machinery: sulfur transfer from the SUFS-SUFE complex to SUFA. *FEBS Lett* 581(7):1362-1368 .
38. Ollagnier-de Choudens S*, et al.* (2003) SufA from *Erwinia chrysanthemi.* Characterization of a scaffold protein required for iron-sulfur cluster assembly. *J Biol Chem* 278(20):17993-18001 .
39. Miroux B & Walker JE (1996) Over-production of proteins in *Escherichia coli*: mutant hosts that allow synthesis of some membrane proteins and globular proteins at high levels. *J Mol Biol* 260(3):289-298.
40. Yoshida A (1970) Enzyme purification by selective elution with substrate analog from ion-exchange columns: application to glucose 6-phosphate dehydrogenase, pseudocholinesterase, lactate dehydrogenase, and alanine dehydrogenase. *Anal Biochem* 37(2):357-367 .
41. Beinert H (1986) Iron-sulphur clusters: agents of electron transfer and storage, and direct participants in enzymic reactions. Tenth Keilin memorial lecture. *Biochem Soc Trans* 14(3):527-533 .
42. Fish WW (1988) Rapid colorimetric micromethod for the quantitation of complexed iron in biological samples. *Methods Enzymol* 158:357-364 .
43. Song SH, Dick B, Penzkofer A, & Hegemann P (2007) Photo-reduction of flavin mononucleotide to semiquinone form in LOV domain mutants of blue-light receptor phot from *Chlamydomonas reinhardtii*. *J Photochem Photobiol B* 87(1):37-48 .
44. Gardner PR & Fridovich I (1992) Inactivation-reactivation of aconitase in *Escherichia coli.* A sensitive measure of superoxide radical. *J Biol Chem* 267(13):8757-8763 .
45. Morbach S, Tebbe S, & Schneider E (1993) The ATP-binding cassette (ABC) transporter for maltose/maltodextrins of *Salmonella typhimurium*. Characterization of the ATPase activity associated with the purified MalK subunit. *J Biol Chem* 268(25):18617-18621 .
46. Miller JH (1972) *Experiments in molecular genetics* (Cold Spring Harbor Laboratory Press) p 468.
47. Vinella D, Loiseau L, Ollagnier de Choudens S, Fontecave M, & Barras F (in preperation) Maturation of IscR and NsrR, two [Fe-S] containing stress regulators in *Escherichia coli.*

48. Vinella D, Brochier-Armanet C, Loiseau L, Talla E, & Barras F (2009) Iron-sulfur (Fe/S) protein biogenesis: phylogenomic and genetic studies of A-type carriers. *PLoS Genet* 5(5):e1000497 .
49. Baba T*, et al.* (2006) Construction of *Escherichia coli K-12* in-frame, single-gene knockout mutants: the Keio collection. *Mol Syst Biol* 2:2006 0008 .
50. Vinella D, Cashel M, & D'Ari R (2000) Selected amplification of the cell division genes ftsQ-ftsA-ftsZ in *Escherichia coli*. *Genetics* 156(4):1483-1492 .
51. Trotter V*, et al.* (2009) The CsdA cysteine desulphurase promotes Fe/S biogenesis by recruiting Suf components and participates to a new sulphur transfer pathway by recruiting CsdL (ex-YgdL), a ubiquitin-modifying-like protein. *Mol Microbiol* 74(6):1527-1542 .
52. Guzman LM, Belin D, Carson MJ, & Beckwith J (1995) Tight regulation, modulation, and high-level expression by vectors containing the arabinose PBAD promoter. *J Bacteriol* 177(14):4121-4130 .
53. Outten FW, Djaman O, & Storz G (2004) A suf operon requirement for Fe-S cluster assembly during iron starvation in *Escherichia coli*. *Mol Microbiol* 52(3):861-872 .
54. Nair M*, et al.* (2004) Solution structure of the bacterial frataxin ortholog, CyaY: mapping the iron binding sites. *Structure* 12(11):2037-2048.
55. Cook JD*, et al.* (2006) Monomeric yeast frataxin is an iron-binding protein. *Biochemistry* 45(25):7767-7777.
56. Foury F, Pastore A, & Trincal M (2007) Acidic residues of yeast frataxin have an essential role in Fe-S cluster assembly. *EMBO Rep* 8(2):194-199.
57. Cupp-Vickery JR, Urbina H, & Vickery LE (2003) Crystal structure of IscS, a cysteine desulfurase from *Escherichia coli*. *J Mol Biol* 330(5):1049-1059.
58. Kaiser JT*, et al.* (2000) Crystal structure of a NifS-like protein from *Thermotoga maritima*: implications for iron sulphur cluster assembly. *J Mol Biol* 297(2):451-464.
59. Zheng L, White RH, Cash VL, & Dean DR (1994) Mechanism for the desulfurization of L-cysteine catalyzed by the nifS gene product. *Biochemistry* 33(15):4714-4720.
60. Nakai Y, Nakai M, Hayashi H, & Kagamiyama H (2001) Nuclear localization of yeast Nfs1p is required for cell survival. *J Biol Chem* 276(11):8314-8320.
61. Tachezy J, Sanchez LB, & Muller M (2001) Mitochondrial type iron-sulfur cluster assembly in the amitochondriate eukaryotes *Trichomonas vaginalis* and *Giardia intestinalis*, as indicated by the phylogeny of IscS. *Mol Biol Evol* 18(10):1919-1928.
62. Agar JN*, et al.* (2000) Modular organization and identification of a mononuclear iron-binding site within the NifU protein. *J Biol Inorg Chem* 5(2):167-177.
63. Garland SA, Hoff K, Vickery LE, & Culotta VC (1999) *Saccharomyces cerevisiae* ISU1 and ISU2: members of a well-conserved gene family for iron-sulfur cluster assembly. *J Mol Biol* 294(4):897-907.
64. Dutkiewicz R*, et al.* (2004) Sequence-specific interaction between mitochondrial Fe-S scaffold protein Isu and Hsp70 Ssq1 is essential for their *in vivo* function. *J Biol Chem* 279(28):29167-29174.

65. Yuvaniyama P, Agar JN, Cash VL, Johnson MK, & Dean DR (2000) NifS-directed assembly of a transient [2Fe-2S] cluster within the NifU protein. *Proc Natl Acad Sci U S A* 97(2):599-604.
66. Boyd JM, Drevland RM, Downs DM, & Graham DE (2009) Archaeal ApbC/Nbp35 homologs function as iron-sulfur cluster carrier proteins. *J Bacteriol* 191(5):1490-1497 .

Fig S1

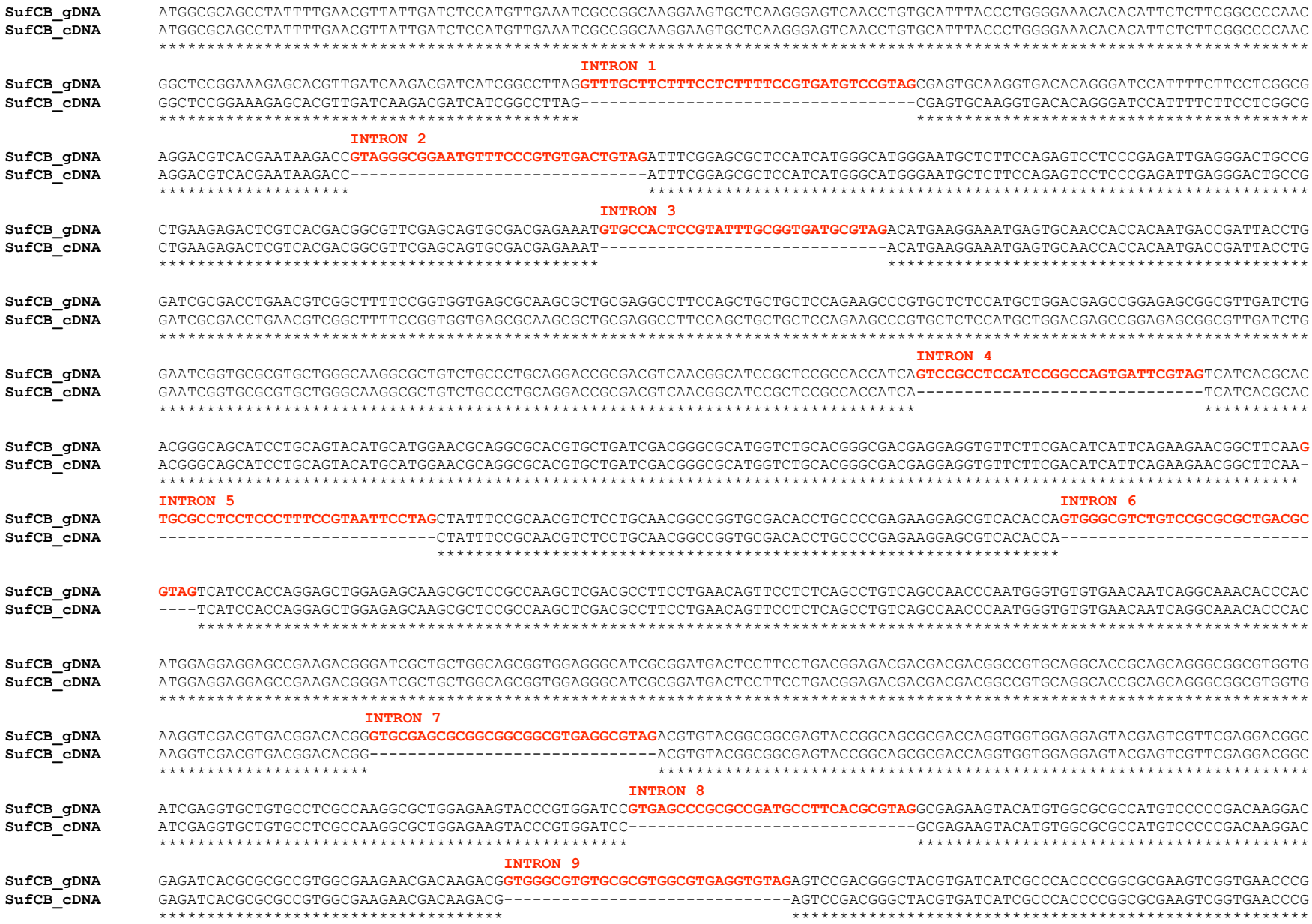
SufCB_gDNA
SufCB_cDNA
INTRON 1
INTRON 2
INTRON 3
INTRON 4
INTRON 5
INTRON 6
INTRON 7
INTRON 8
INTRON 9

```
SufCB_gDNA      ATCAACAGCCAGCTGATCATGGAGAACAACAAGATCCAGTACGTGCACAACATCCTCATCTCCATGCCCGGCTCCTGTCTGACCGTCGCCTCGCTCTGCACCTACCACTGCGGCCAGAAG
SufCB_cDNA      ATCAACAGCCAGCTGATCATGGAGAACAACAAGATCCAGTACGTGCACAACATCCTCATCTCCATGCCCGGCTCCTGTCTGACCGTCGCCTCGCTCTGCACCTACCACTGCGGCCAGAAG
                ********************************************************************************************************************

                                                                                                  INTRON 10
SufCB_gDNA      GACCACCACGACTACATCGTCGGCGGGCAGCACTACGGCGTGTCCGAGTTCTTCGTGGAGAAGGACTCGGAGCTCTGCTTCTCGATGGTTTGGGTTCTGCTCCTTGTTTACCGCAGATTC
SufCB_cDNA      GACCACCACGACTACATCGTCGGCGGGCAGCACTACGGCGTGTCCGAGTTCTTCGTGGAGAAGGACTCGGAGCTCTGCTTCTCGATG----------------------------ATTC
                ********************************************************************************                                ****

SufCB_gDNA      ACACGTGGTGCAACTCCTACATCGTGTGGCCGCGCTCCGCCGCCGTCGTGGAGGAGAACGGCGTGTTCTACTCCAACTACGTGTGTTTGGAGCCCGTGGTCAAGGTCCAGATGTGCCCCG
SufCB_cDNA      ACACGTGGTGCAACTCCTACATCGTGTGGCCGCGCTCCGCCGCCGTCGTGGAGGAGAACGGCGTGTTCTACTCCAACTACGTGTGTTTGGAGCCCGTGGTCAAGGTCCAGATGTGCCCCG
                ********************************************************************************************************************

SufCB_gDNA      TGGCCGACCTGCGCGGGCGCAACGCCGTGGCGAAGTTCAGCGCGGTGCTGCTGGCGAAGGAGGGCACGACGCTGGACGTGGGGTCGCGCGCGTTGCTGAATGCCGAGGGTGCGCGCAGCG
SufCB_cDNA      TGGCCGACCTGCGCGGGCGCAACGCCGTGGCGAAGTTCAGCGCGGTGCTGCTGGCGAAGGAGGGCACGACGCTGGACGTGGGGTCGCGCGCGTTGCTGAATGCCGAGGGTGCGCGCAGCG
                ********************************************************************************************************************

SufCB_gDNA      AGAGCATCACGCGCACCATCTCGAAGGGTGGCGTGATCTTCGCGCGCGCGGACATCCAGGGCAACGCGCTGAACACGAAGGGACACATCGAGTGCCAGGGTCTGGTGGTGGACGAGGGTA
SufCB_cDNA      AGAGCATCACGCGCACCATCTCGAAGGGTGGCGTGATCTTCGCGCGCGCGGACATCCAGGGCAACGCGCTGAACACGAAGGGACACATCGAGTGCCAGGGTCTGGTGGTGGACGAGGGTA
                ********************************************************************************************************************

SufCB_gDNA      AGGGCGTGATCCACTCGATTCCGCAGATCTCGGGCAGCTTCGGCACGGAGCTGAGCCACGAGGCGGCGATCGGCCGGATCGCGAAGGACAAGATCGAGTACCTGATGACGCGCCGCATGA
SufCB_cDNA      AGGGCGTGATCCACTCGATTCCGCAGATCTCGGGCAGCTTCGGCACGGAGCTGAGCCACGAGGCGGCGATCGGCCGGATCGCGAAGGACAAGATCGAGTACCTGATGACGCGCCGCATGA
                ********************************************************************************************************************

SufCB_gDNA      CGGAGGAGGAGGCAGTGTCGGTGATCATCCGCGGTTTCCTGAACGTGAAGGTGCAGGGCATTCCGAAGTCGATCCAGCAGCAGATGGACGAGATCATCGACCAGGCGAGCAAGGAGGGGT
SufCB_cDNA      CGGAGGAGGAGGCAGTGTCGGTGATCATCCGCGGTTTCCTGAACGTGAAGGTGCAGGGCATTCCGAAGTCGATCCAGCAGCAGATGGACGAGATCATCGACCAGGCGAGCAAGGAGGGGT
                ********************************************************************************************************************

SufCB_gDNA      TCTGA
SufCB_cDNA      TCTGA
                *****
```

Fig S2

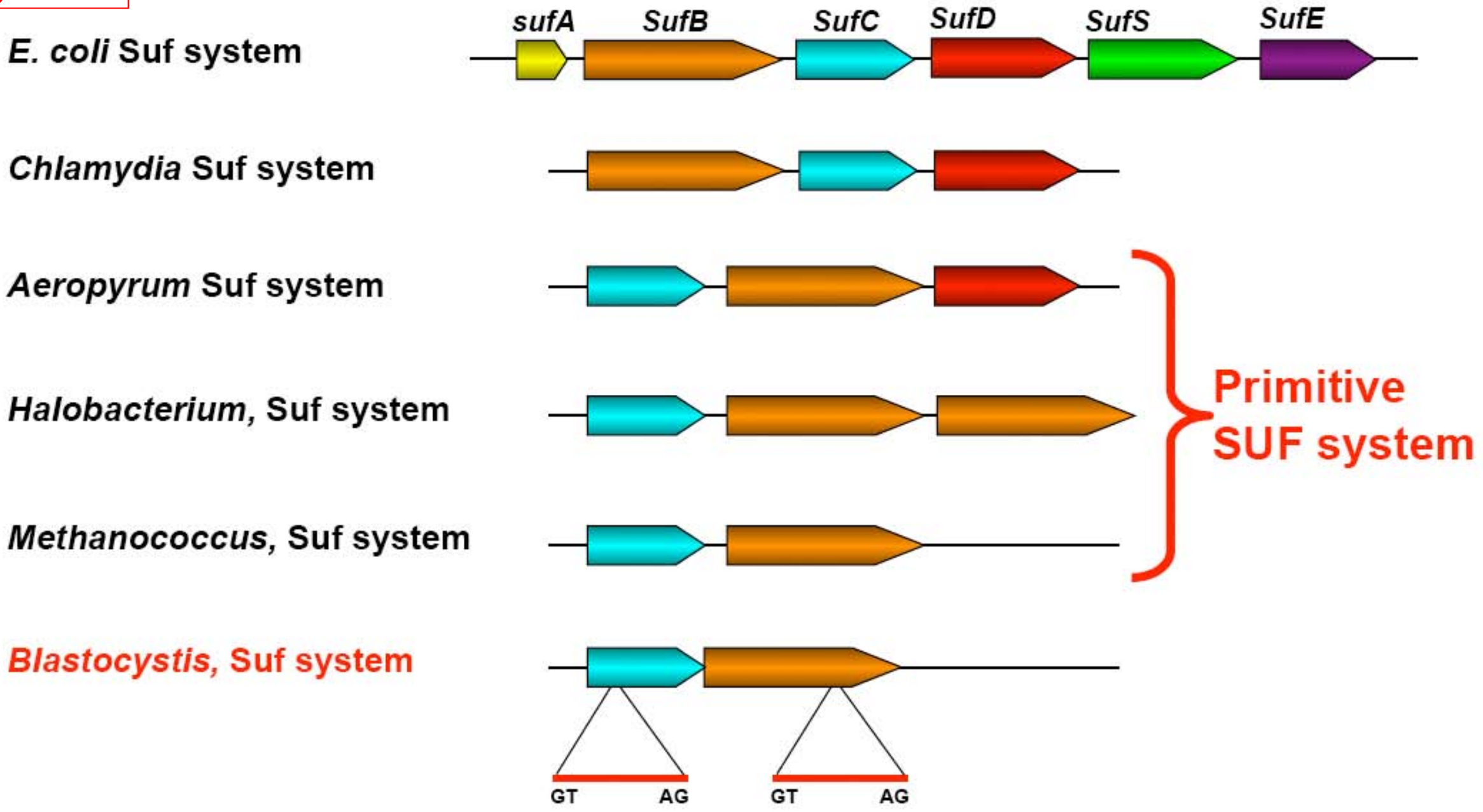
E. coli Suf system
sufA
SufB
SufC
SufD
SufS
SufE
Chlamydia Suf system
Aeropyrum Suf system
Halobacterium, Suf system
Methanococcus, Suf system
Primitive
SUF system
Blastocystis, Suf system
GT
AG
GT
AG

Fig S3

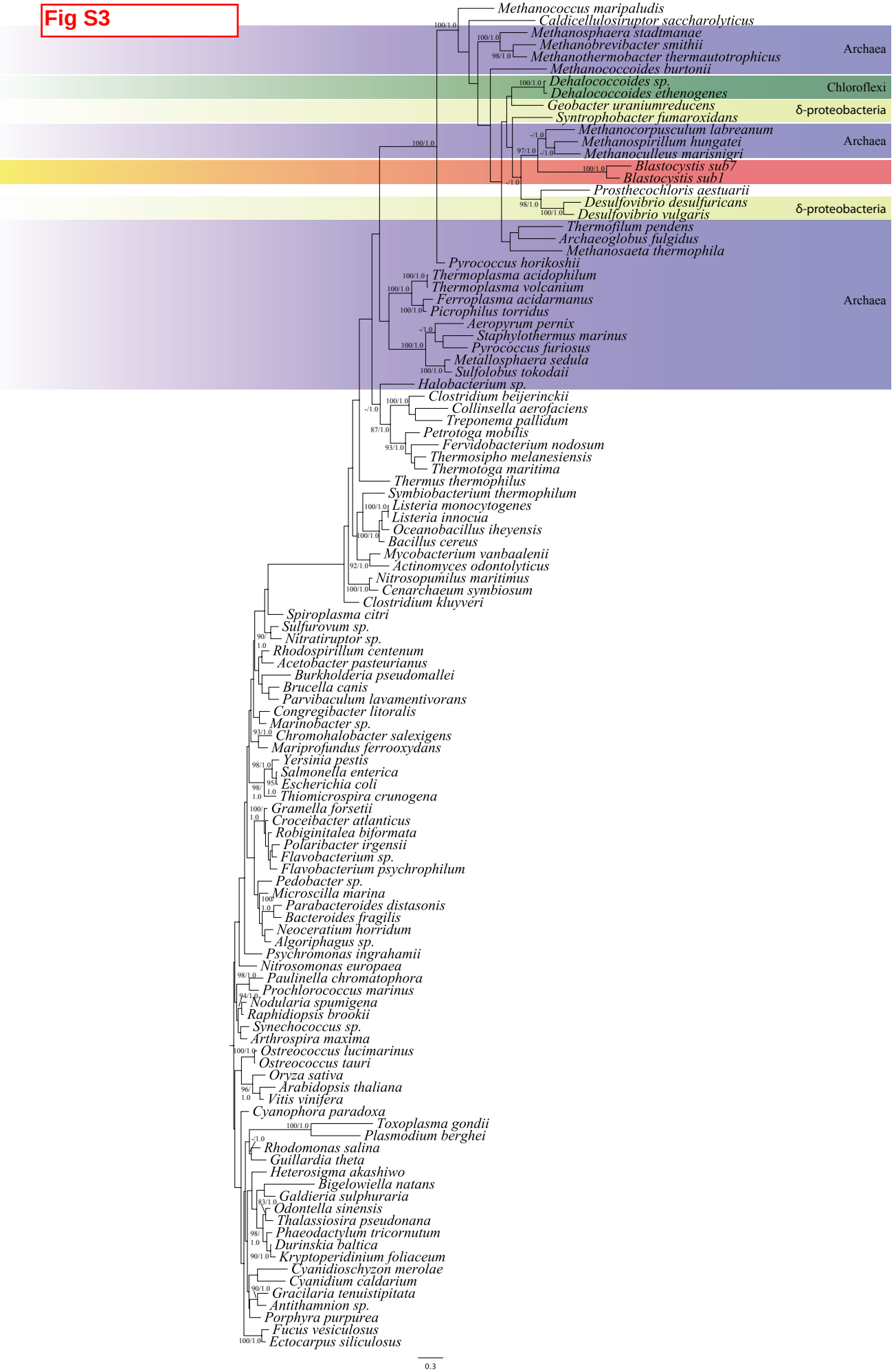
Methanococcus maripaludis
Caldicellulosiruptor saccharolyticus
Methanosphaera stadtmanae
Methanobrevibacter smithii
Methanothermobacter thermautotrophicus
Archaea
Methanococcoides burtonii
Dehalococcoides sp.
Dehalococcoides ethenogenes
Chloroflexi
Geobacter uraniumreducens
Syntrophobacter fumaroxidans
δ-proteobacteria
Methanocorpusculum labreanum
Methanospirillum hungatei
Methanoculleus marisnigri
Archaea
Blastocystis sub7
Blastocystis sub1
Prosthecochloris aestuarii
Desulfovibrio desulfuricans
Desulfovibrio vulgaris
δ-proteobacteria
Thermofilum pendens
Archaeoglobus fulgidus
Methanosaeta thermophila
Pyrococcus horikoshii
Thermoplasma acidophilum
Thermoplasma volcanium
Ferroplasma acidarmanus
Picrophilus torridus
Archaea
Aeropyrum pernix
Staphylothermus marinus
Pyrococcus furiosus
Metallosphaera sedula
Sulfolobus tokodaii
Halobacterium sp.
Clostridium beijerinckii
Collinsella aerofaciens
Treponema pallidum
Petrotoga mobilis
Fervidobacterium nodosum
Thermosipho melanesiensis
Thermotoga maritima
Thermus thermophilus
Symbiobacterium thermophilum
Listeria monocytogenes
Listeria innocua
Oceanobacillus iheyensis
Bacillus cereus
Mycobacterium vanbaalenii
Actinomyces odontolyticus
Nitrosopumilus maritimus
Cenarchaeum symbiosum
Clostridium kluyveri
Spiroplasma citri
Sulfurovum sp.
Nitratiruptor sp.
Rhodospirillum centenum
Acetobacter pasteurianus
Burkholderia pseudomallei
Brucella canis
Parvibaculum lavamentivorans
Congregibacter litoralis
Marinobacter sp.
Chromohalobacter salexigens
Mariprofundus ferrooxydans
Yersinia pestis
Salmonella enterica
Escherichia coli
Thiomicrospira crunogena
Gramella forsetii
Croceibacter atlanticus
Robiginitalea biformata
Polaribacter irgensii
Flavobacterium sp.
Flavobacterium psychrophilum
Pedobacter sp.
Microscilla marina
Parabacteroides distasonis
Bacteroides fragilis
Neoceratium horridum
Algoriphagus sp.
Psychromonas ingrahamii
Nitrosomonas europaea
Paulinella chromatophora
Prochlorococcus marinus
Nodularia spumigena
Raphidiopsis brookii
Synechococcus sp.
Arthrospira maxima
Ostreococcus lucimarinus
Ostreococcus tauri
Oryza sativa
Arabidopsis thaliana
Vitis vinifera
Cyanophora paradoxa
Toxoplasma gondii
Plasmodium berghei
Rhodomonas salina
Guillardia theta
Heterosigma akashiwo
Bigelowiella natans
Galdieria sulphuraria
Odontella sinensis
Thalassiosira pseudonana
Phaeodactylum tricornutum
Durinskia baltica
Kryptoperidinium foliaceum
Cyanidioschyzon merolae
Cyanidium caldarium
Gracilaria tenuistipitata
Antithamnion sp.
Porphyra purpurea
Fucus vesiculosus
Ectocarpus siliculosus
0.3

Fig S4

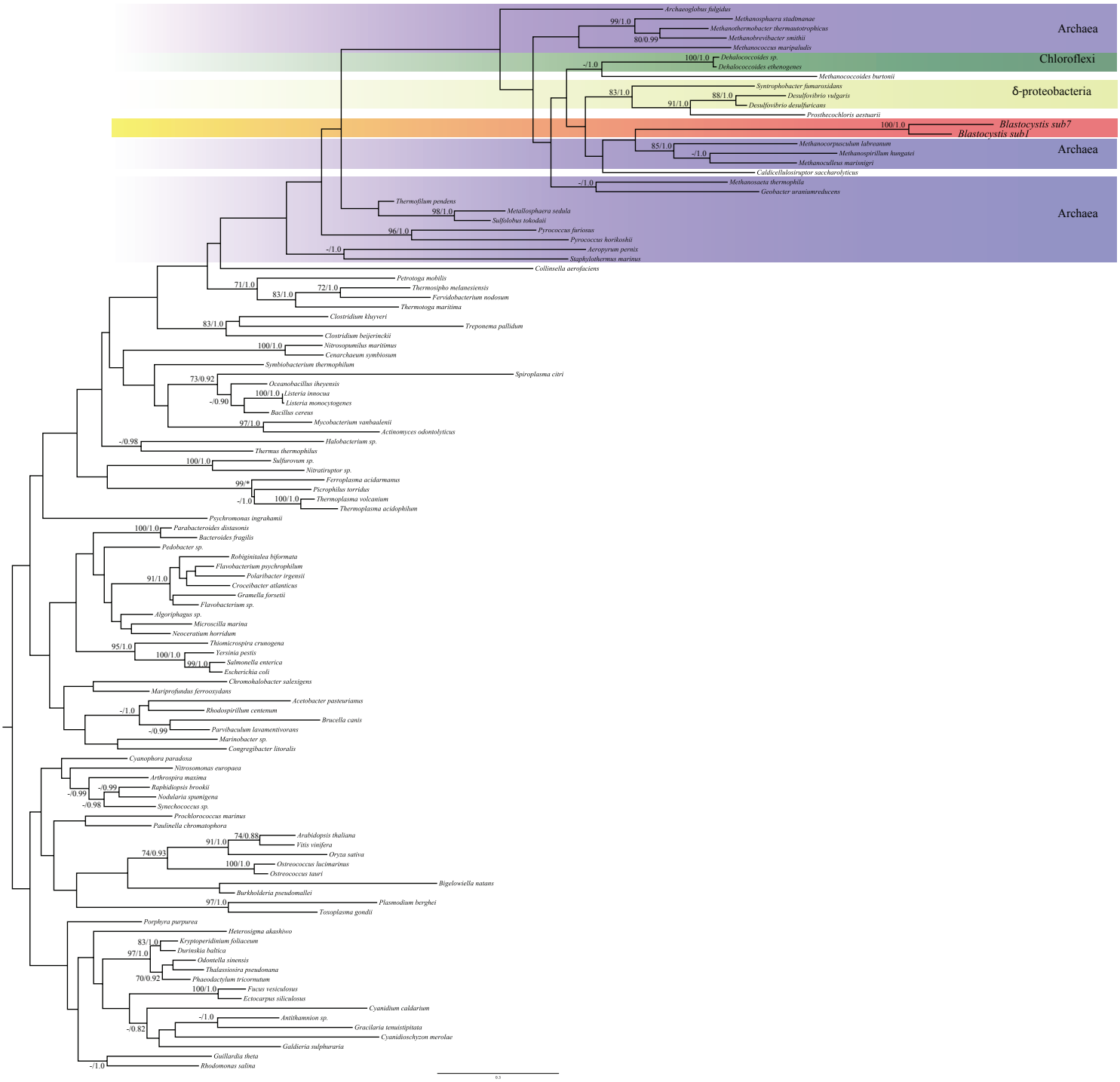
Archaeoglobus fulgidus
Methanosphaera stadtmanae
Methanothermobacter thermautotrophicus
Methanobrevibacter smithii
Methanococcus maripaludis
Archaea
Dehalococcoides sp.
Dehalococcoides ethenogenes
Chloroflexi
Methanococcoides burtonii
Syntrophobacter fumaroxidans
Desulfovibrio vulgaris
Desulfovibrio desulfuricans
δ-proteobacteria
Prosthecochloris aestuarii
Blastocystis sub7
Blastocystis sub1
Methanocorpusculum labreanum
Methanospirillum hungatei
Methanoculleus marisnigri
Archaea
Caldicellulosiruptor saccharolyticus
Methanosaeta thermophila
Geobacter uraniumreducens
Thermofilum pendens
Metallosphaera sedula
Sulfolobus tokodaii
Pyrococcus furiosus
Pyrococcus horikoshii
Aeropyrum pernix
Staphylothermus marinus
Archaea
Collinsella aerofaciens
Petrotoga mobilis
Thermospho melanesiensis
Fervidobacterium nodosum
Thermotoga maritima
Clostridium kluyveri
Treponema pallidum
Clostridium beijerinckii
Nitrosopumilus maritimus
Cenarchaeum symbiosum
Symbiobacterium thermophilum
Spiroplasma citri
Oceanobacillus iheyensis
Listeria innocua
Listeria monocytogenes
Bacillus cereus
Mycobacterium vanbaalenii
Actinomyces odontolyticus
Halobacterium sp.
Thermus thermophilus
Sulfurovum sp.
Nitratiruptor sp.
Ferroplasma acidarmanus
Picrophilus torridus
Thermoplasma volcanium
Thermoplasma acidophilum
Psychromonas ingrahamii
Parabacteroides distasonis
Bacteroides fragilis
Pedobacter sp.
Robiginitalea biformata
Flavobacterium psychrophilum
Polaribacter irgensii
Croceibacter atlanticus
Gramella forsetii
Flavobacterium sp.
Algoriphagus sp.
Microscilla marina
Neoceratium horridum
Thiomicrospira crunogena
Yersinia pestis
Salmonella enterica
Escherichia coli
Chromohalobacter salexigens
Mariprofundus ferrooxydans
Acetobacter pasteurianus
Rhodospirillum centenum
Brucella canis
Parvibaculum lavamentivorans
Marinobacter sp.
Congregibacter litoralis
Cyanophora paradoxa
Nitrosomonas europaea
Arthrospira maxima
Rapidiagnis brookii
Nodularia spumigena
Synechococcus sp.
Prochlorococcus marinus
Paulinella chromatophora
Arabidopsis thaliana
Vitis vinifera
Oryza sativa
Ostreococcus lucimarinus
Ostreococcus tauri
Bigelowiella natans
Burkholderia pseudomallei
Plasmodium berghei
Toxoplasma gondii
Porphyra purpurea
Heterosigma akashiwo
Kryptoperidinium foliaceum
Durinskia baltica
Odontella sinensis
Thalassiosira pseudonana
Phaeodactylum tricornutum
Fucus vesiculosus
Ectocarpus siliculosus
Cyanidium caldarium
Antithamnion sp.
Gracilaria tenuistipitata
Cyanidioschyzon merolae
Galdieria sulphuraria
Guillardia theta
Rhodomonas salina
0.5

Fig S5

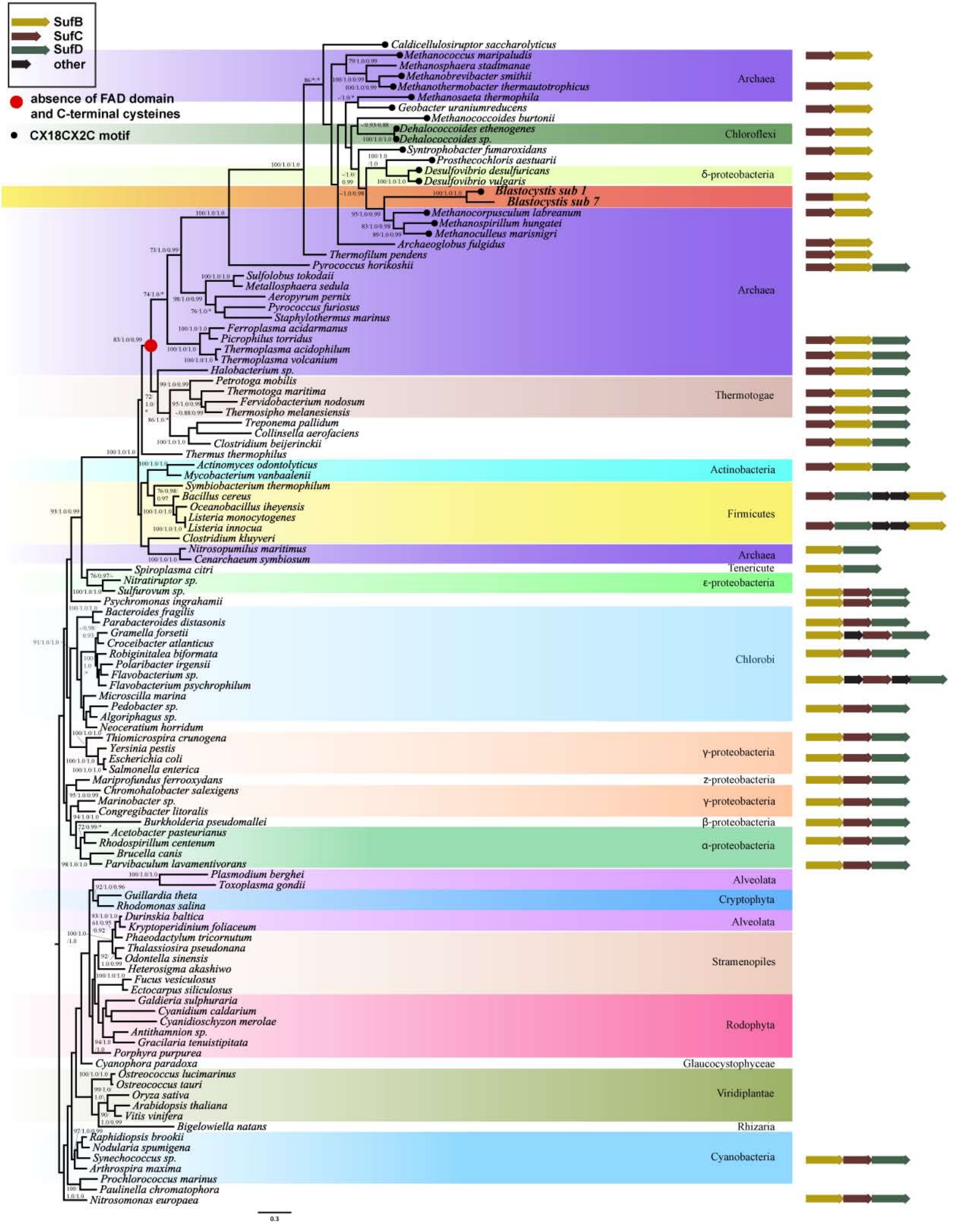
SufB
SufC
SufD
other
absence of FAD domain and C-terminal cysteines
CX18CX2C motif
Caldicellulosiruptor saccharolyticus
Methanococcus maripaludis
Methanosphaera stadtmanae
Methanobrevibacter smithii
Methanothermobacter thermautotrophicus
Methanosaeta thermophila
Geobacter uraniumreducens
Methanococcoides burtonii
Dehalococcoides ethenogenes
Dehalococcoides sp.
Syntrophobacter fumaroxidans
Prosthecochloris aestuarii
Desulfovibrio desulfuricans
Desulfovibrio vulgaris
Blastocystis sub 1
Blastocystis sub 7
Methanocorpusculum labreanum
Methanospirillum hungatei
Methanoculleus marisnigri
Archaeoglobus fulgidus
Thermofilum pendens
Pyrococcus horikoshii
Sulfolobus tokodaii
Metallosphaera sedula
Aeropyrum pernix
Pyrococcus furiosus
Staphylothermus marinus
Ferroplasma acidarmanus
Picrophilus torridus
Thermoplasma acidophilum
Thermoplasma volcanium
Halobacterium sp.
Petrotoga mobilis
Thermotoga maritima
Fervidobacterium nodosum
Thermosipho melanesiensis
Treponema pallidum
Collinsella aerofaciens
Clostridium beijerinckii
Thermus thermophilus
Actinomyces odontolyticus
Mycobacterium vanbaalenii
Symbiobacterium thermophilum
Bacillus cereus
Oceanobacillus iheyensis
Listeria monocytogenes
Listeria innocua
Clostridium kluyveri
Nitrosopumilus maritimus
Cenarchaeum symbiosum
Spiroplasma citri
Nitratiruptor sp.
Sulfurovum sp.
Psychromonas ingrahamii
Bacteroides fragilis
Parabacteroides distasonis
Gramella forsetii
Croceibacter atlanticus
Robiginitalea biformata
Polaribacter irgensii
Flavobacterium sp.
Flavobacterium psychrophilum
Microscilla marina
Pedobacter sp.
Algoriphagus sp.
Neoceratium horridum
Thiomicrospira crunogena
Yersinia pestis
Escherichia coli
Salmonella enterica
Mariprofundus ferrooxydans
Chromohalobacter salexigens
Marinobacter sp.
Congregibacter litoralis
Burkholderia pseudomallei
Acetobacter pasteurianus
Rhodospirillum centenum
Brucella canis
Parvibaculum lavamentivorans
Plasmodium berghei
Toxoplasma gondii
Guillardia theta
Rhodomonas salina
Durinskia baltica
Kryptoperidinium foliaceum
Phaeodactylum tricornutum
Thalassiosira pseudonana
Odontella sinensis
Heterosigma akashiwo
Fucus vesiculosus
Ectocarpus siliculosus
Galdieria sulphuraria
Cyanidium caldarium
Cyanidioschyzon merolae
Antithamnion sp.
Gracilaria tenuistipitata
Porphyra purpurea
Cyanophora paradoxa
Ostreococcus lucimarinus
Ostreococcus tauri
Oryza sativa
Arabidopsis thaliana
Vitis vinifera
Bigelowiella natans
Raphidiopsis brookii
Nodularia spumigena
Synechococcus sp.
Arthrospira maxima
Prochlorococcus marinus
Paulinella chromatophora
Nitrosomonas europaea
Archaea
Chloroflexi
δ-proteobacteria
Archaea
Thermotogae
Actinobacteria
Firmicutes
Archaea
Tenericute
ε-proteobacteria
Chlorobi
γ-proteobacteria
z-proteobacteria
γ-proteobacteria
β-proteobacteria
α-proteobacteria
Alveolata
Cryptophyta
Alveolata
Stramenopiles
Rodophyta
Glaucocystophyceae
Viridiplantae
Rhizaria
Cyanobacteria
0.3

Fig S6

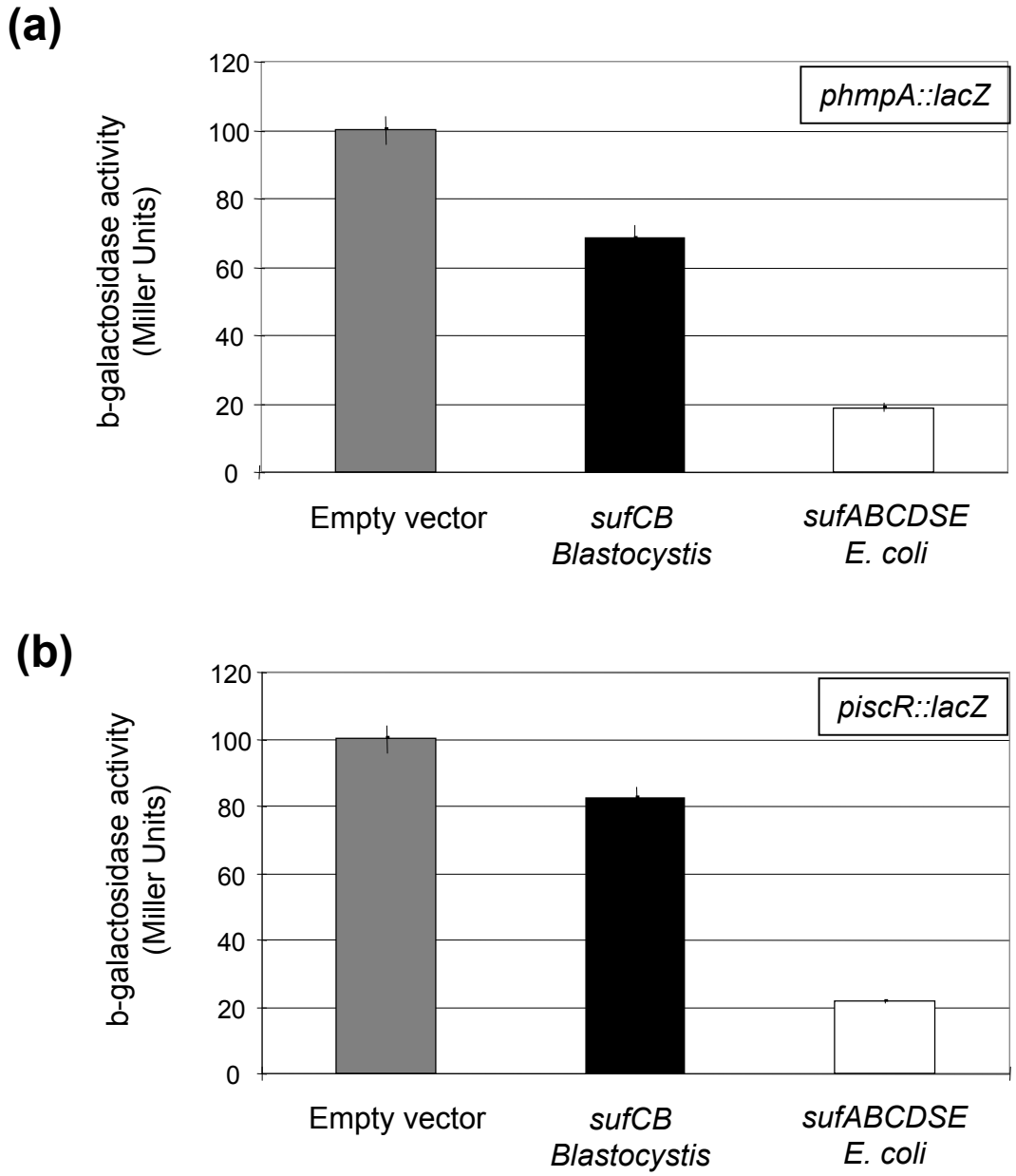
(a)
b-galactosidase activity (Miller Units)
120
100
80
60
40
20
0
phmpA::lacZ
Empty vector
sufCB Blastocystis
sufABCDSE E. coli
(b)
b-galactosidase activity (Miller Units)
120
100
80
60
40
20
0
piscR::lacZ
Empty vector
sufCB Blastocystis
sufABCDSE E. coli

Fig S7

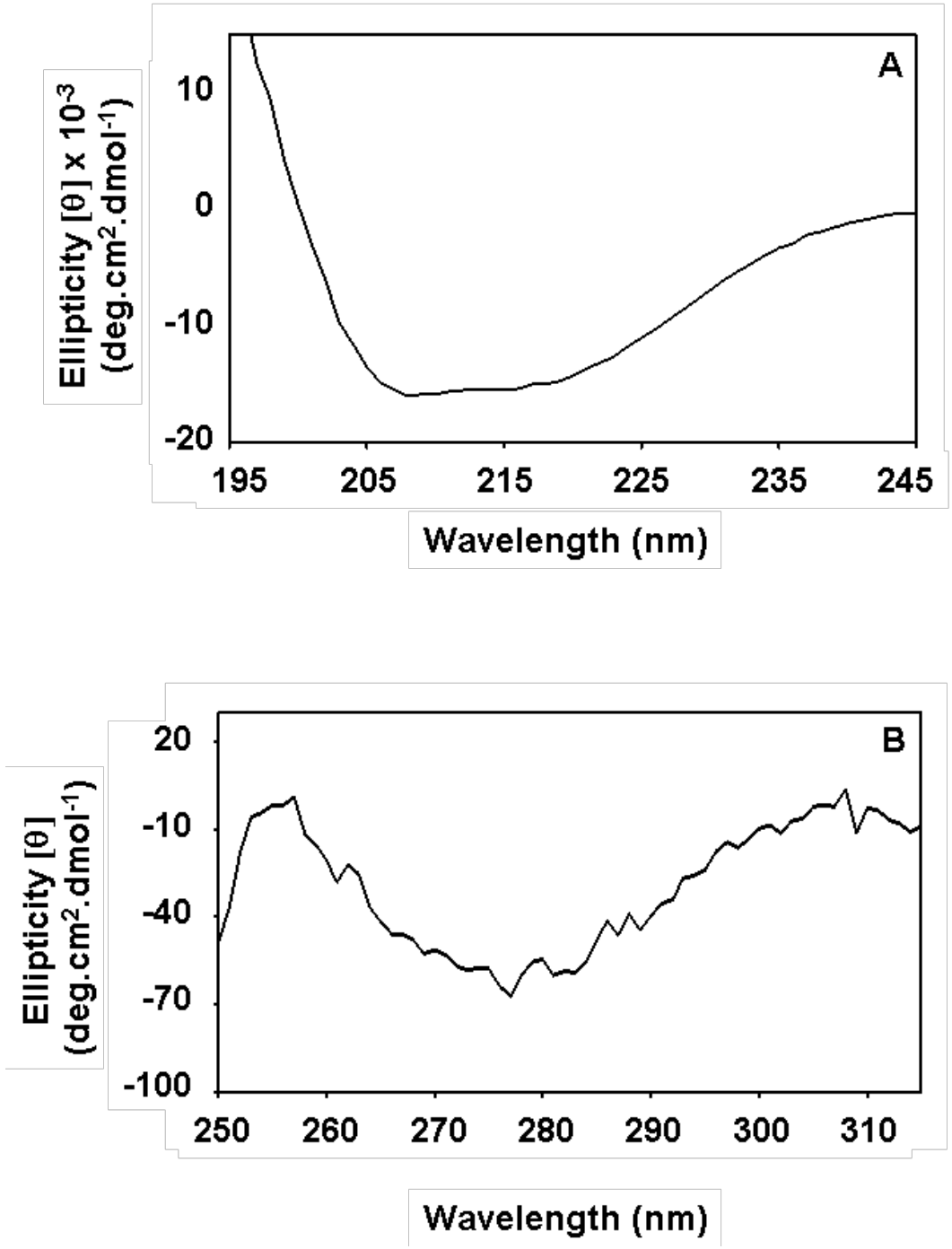
A
10
0
-10
-20
195
205
215
225
235
245
Ellipticity [θ] x 10-3
(deg.cm2.dmol-1)
Wavelength (nm)
B
20
-10
-40
-70
-100
250
260
270
280
290
300
310
Ellipticity [θ]
(deg.cm2.dmol-1)
Wavelength (nm)

Fig S8

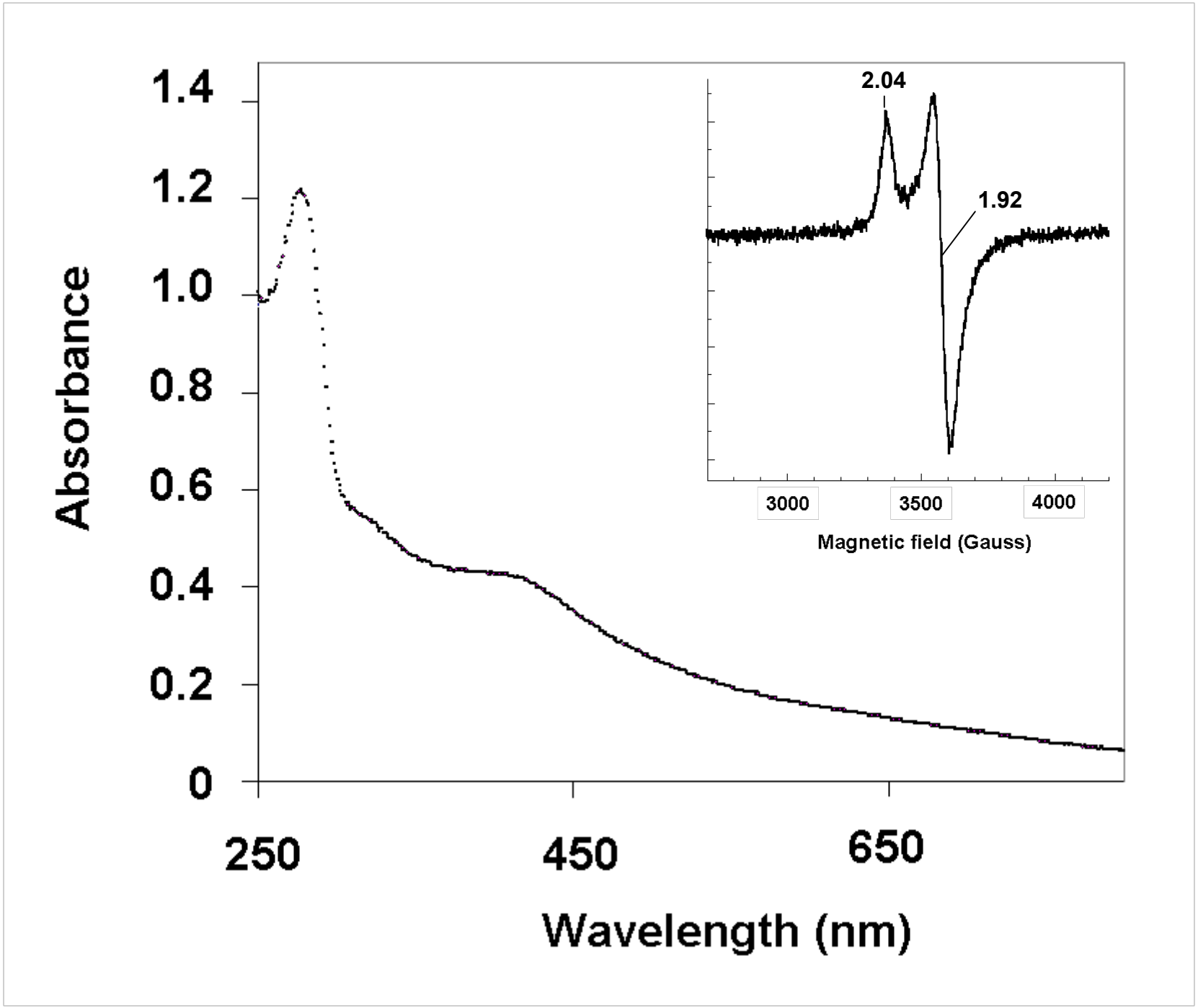
Absorbance
1.4
1.2
1.0
0.8
0.6
0.4
0.2
0
250
450
650
Wavelength (nm)
2.04
1.92
3000
3500
4000
Magnetic field (Gauss)

Fig S9

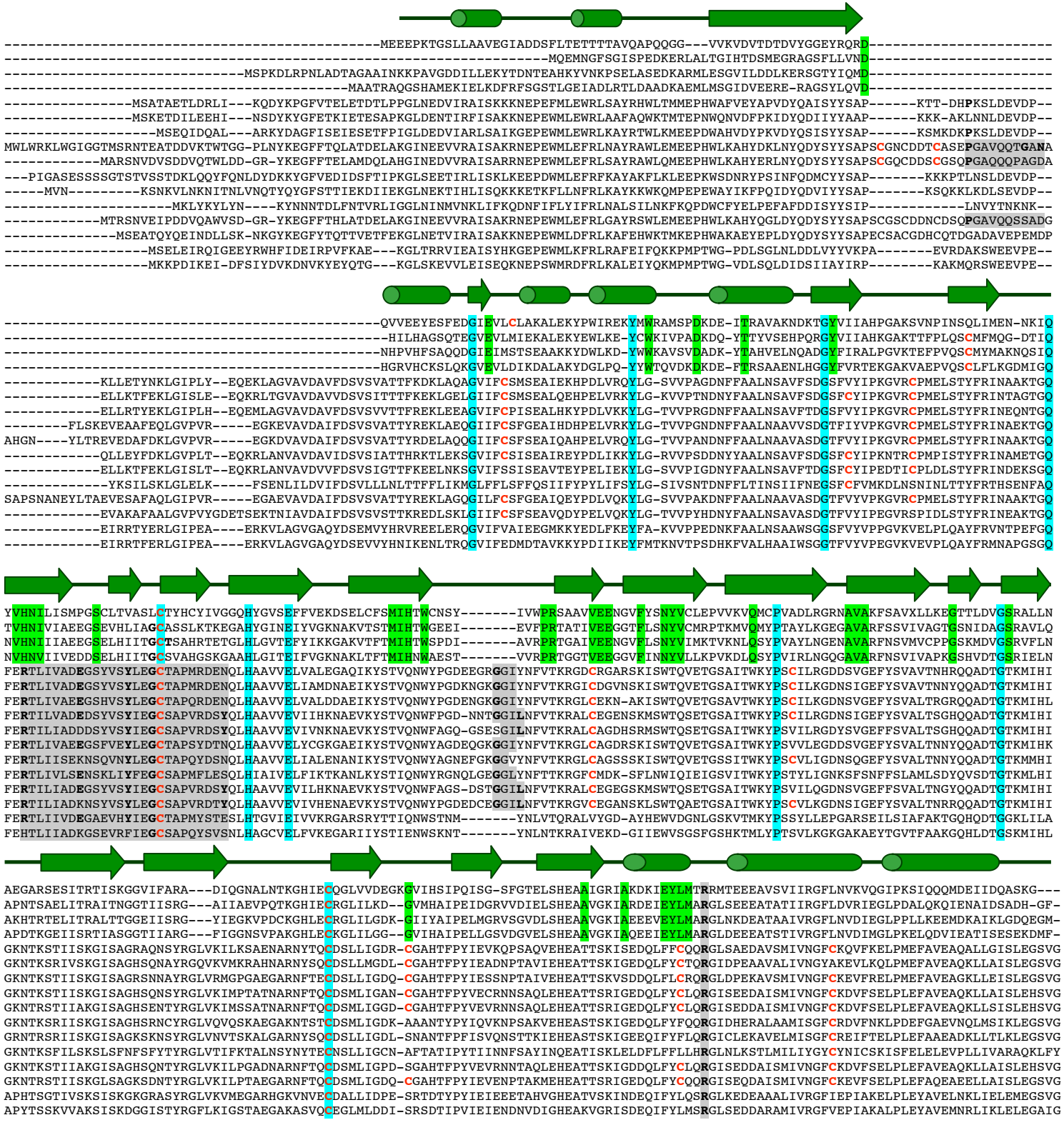
Blastocystis
Methanocorpusculum
Dehalococcoides
Desulfovibrio
Methylococcus
Microscilla marina
Idiomarina loihiensis
Escherichia coli
Erwinia chrysanthemi
Arabidopsis thaliana
Phaeodactylum
Toxoplasma gondii
Yersinia
Thiomicrospira
Thermus thermophilus
Thermoanaerobacter

Fig S10

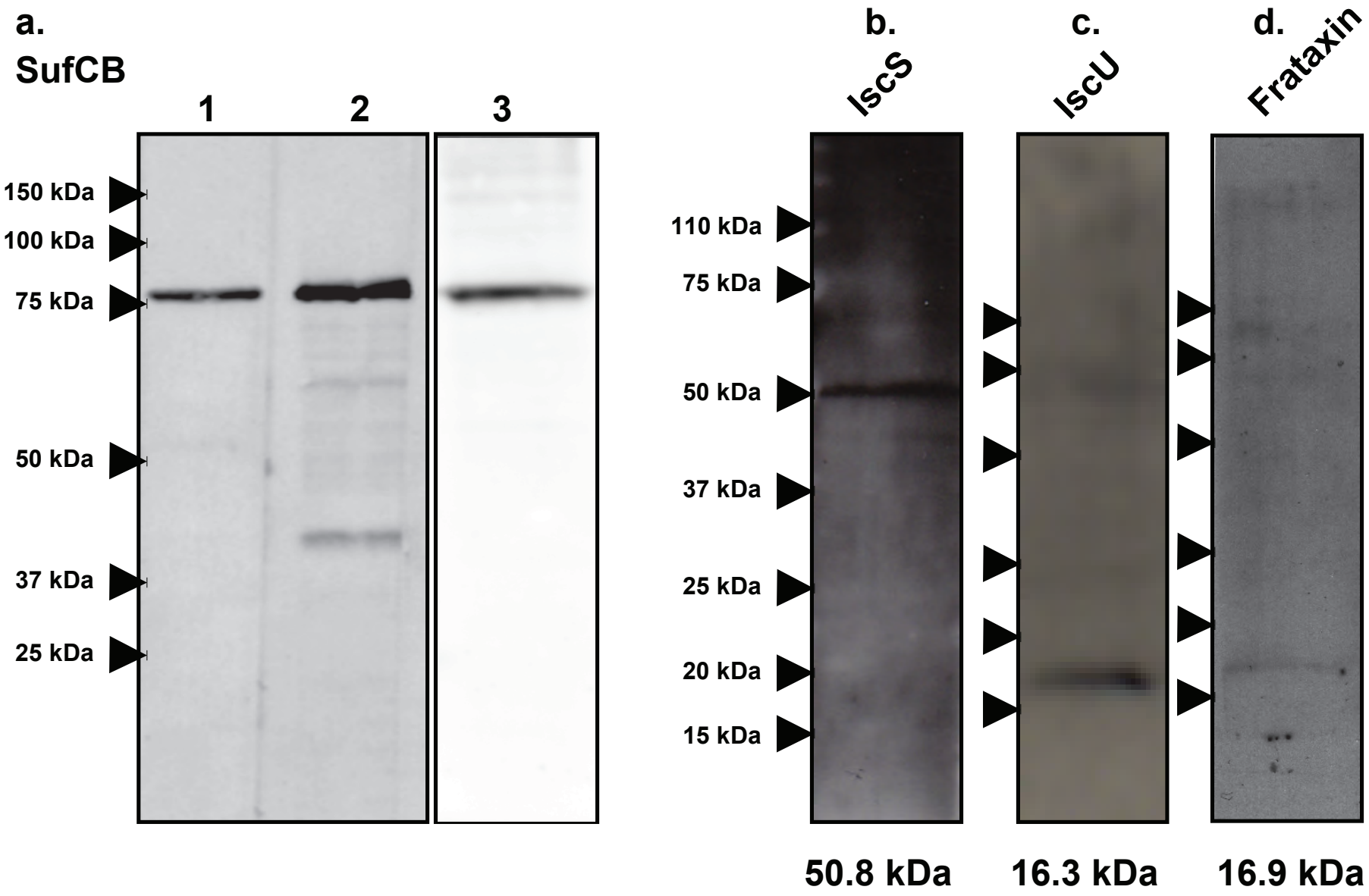

1: Anti-His-Tag antibody against *E. coli* expressing *Blastocystis* SufCB

2: Anti-SufC antisera against *E. coli* expressing *Blastocystis* SufCB

3: Anti-SufC antisera against *Blastocystis* total protein extracts

e.

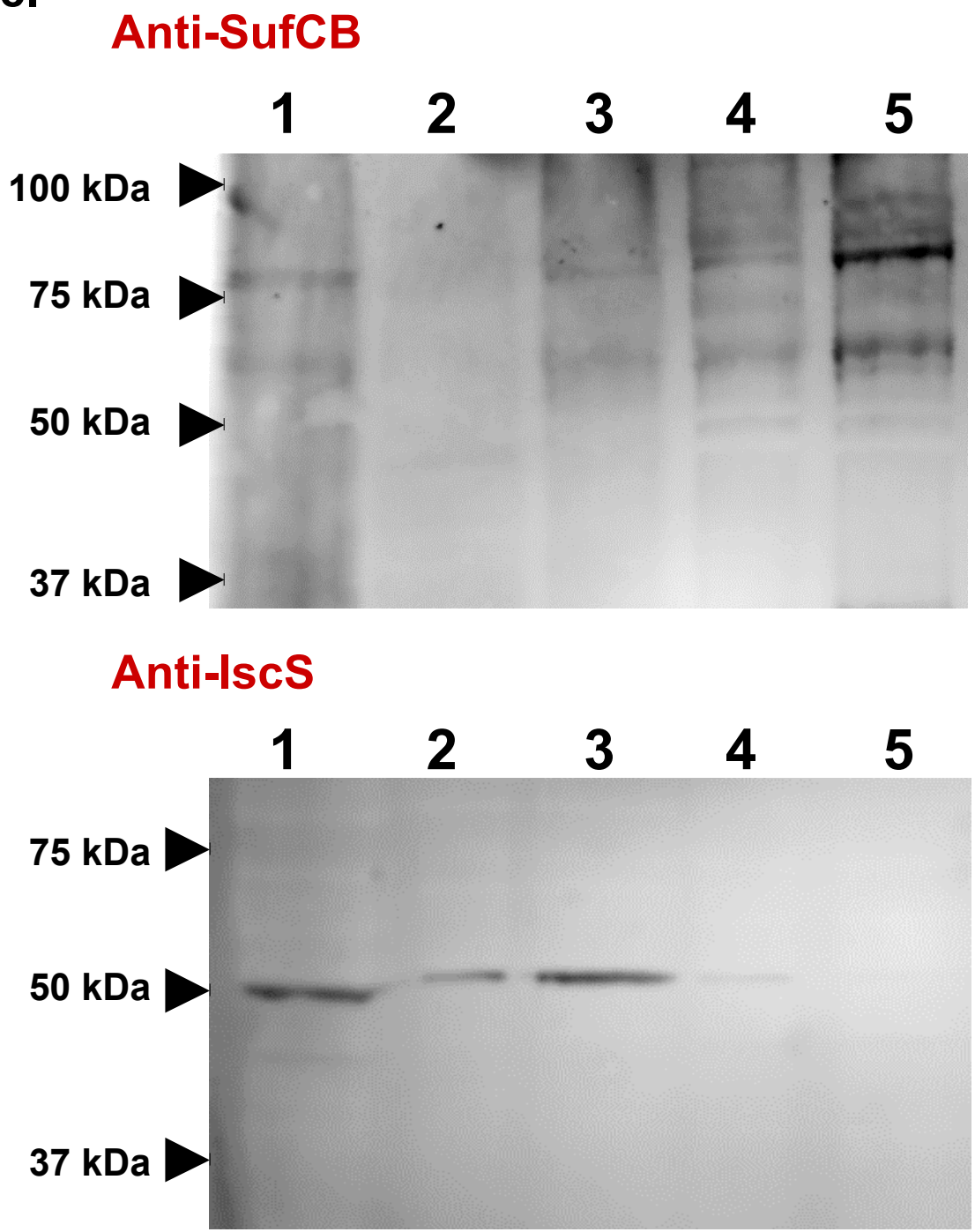

1. Whole cells
2. Large Granule Fraction (LGF) after sucrose gradient
3. LGF before gradient
4. Small Granule fraction (SGF)
5. Cytosolic fraction (supernatant after SGF)

Fig S11

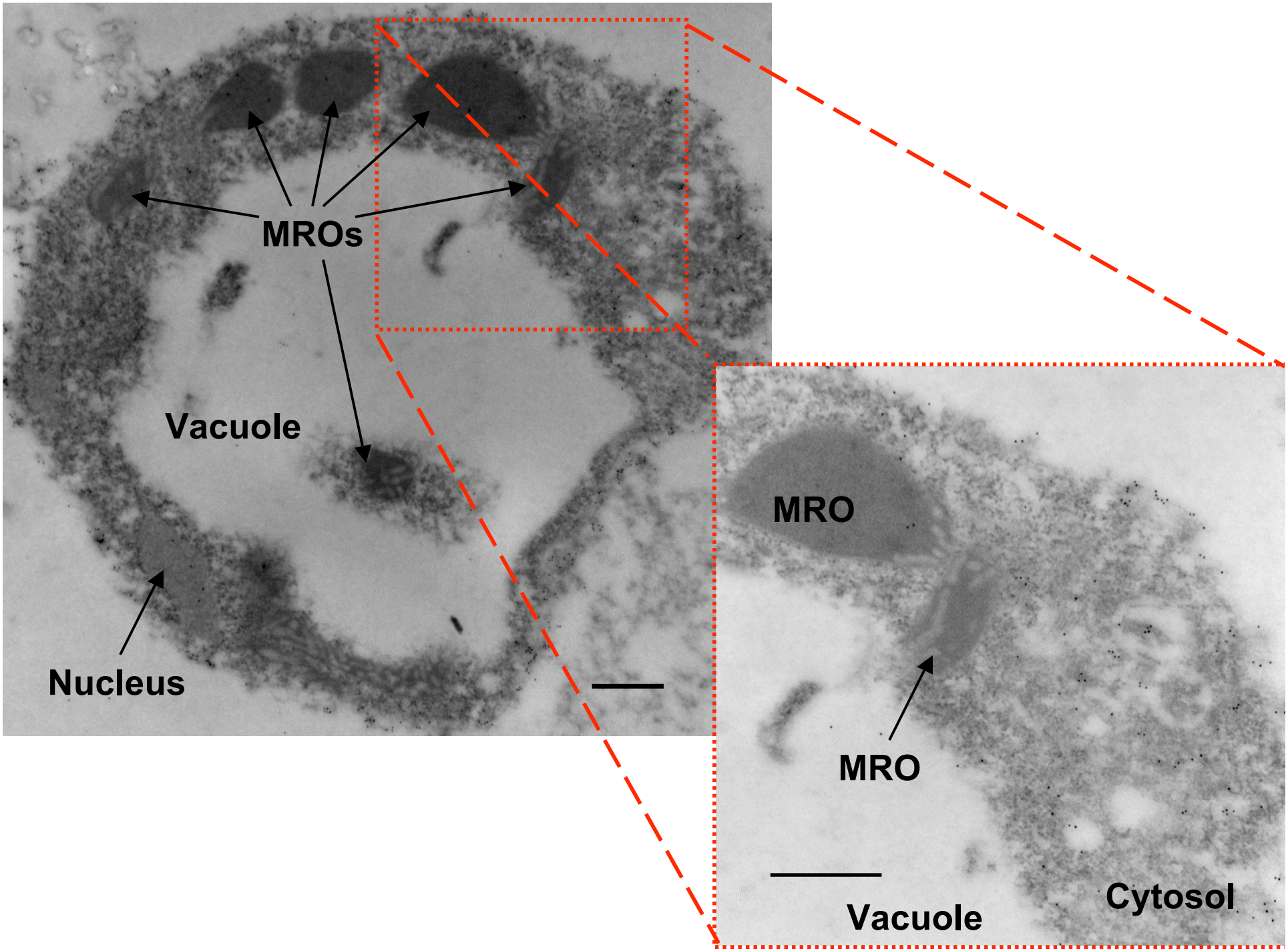

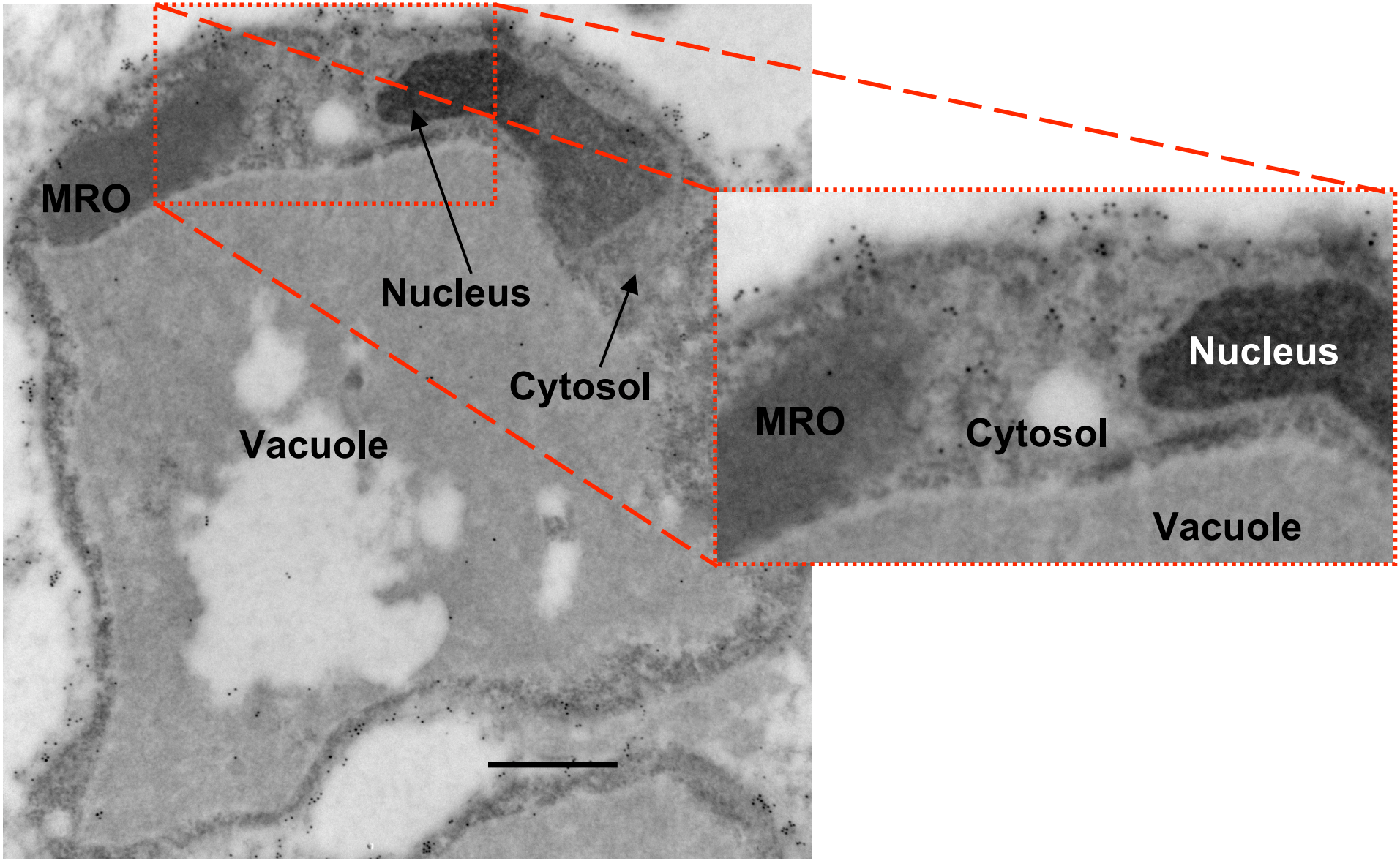
MRO
Nucleus
Cytosol
Vacuole
Nucleus
MRO
Cytosol
Vacuole

Fig S12

anti-IscU

Mitotracker

merged

DIC

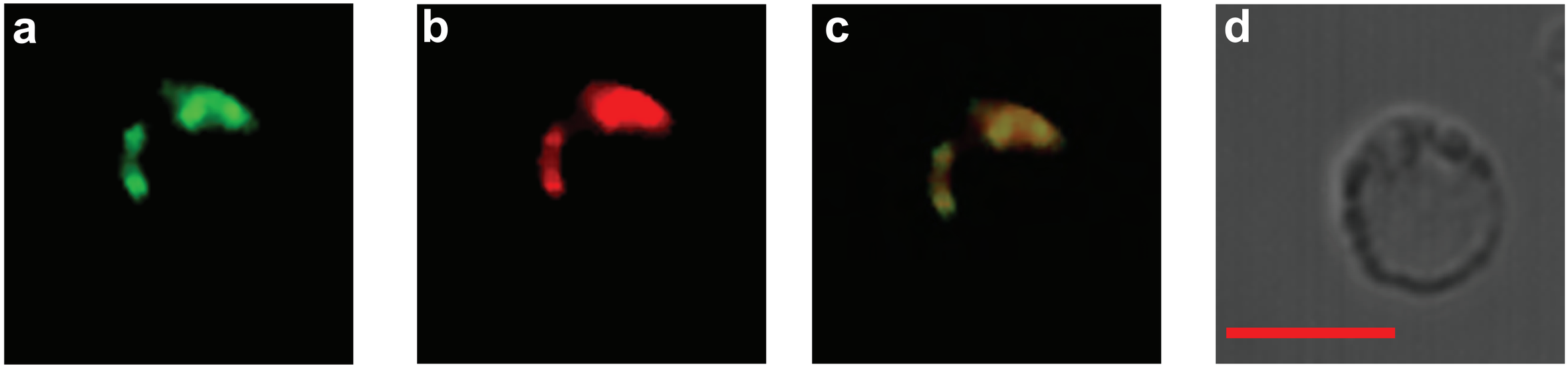

anti-Frataxin

Mitotracker

merged

DIC

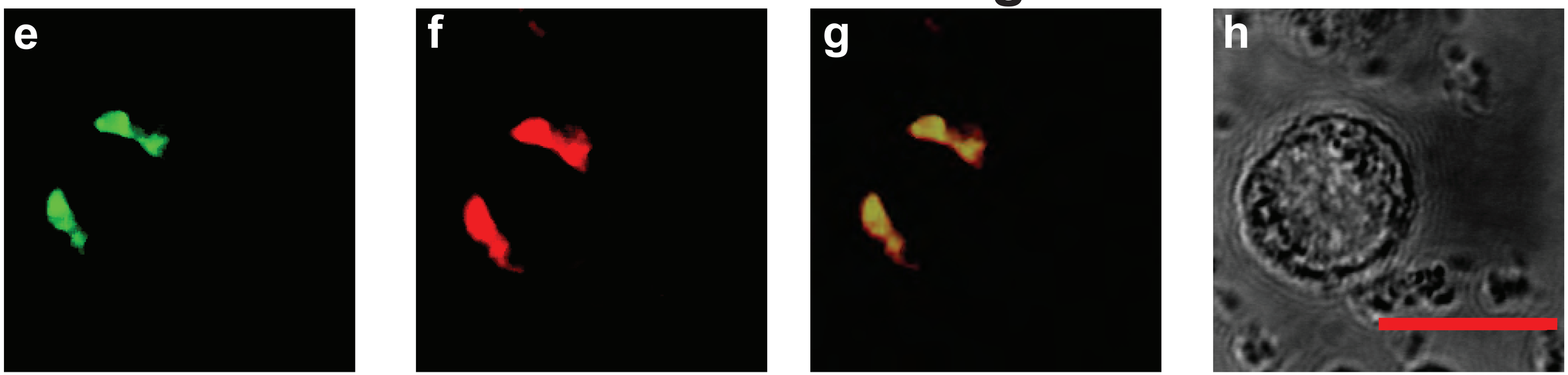

Fig S13

Conservation and identification of functional residues of *Blastocystis* frataxin

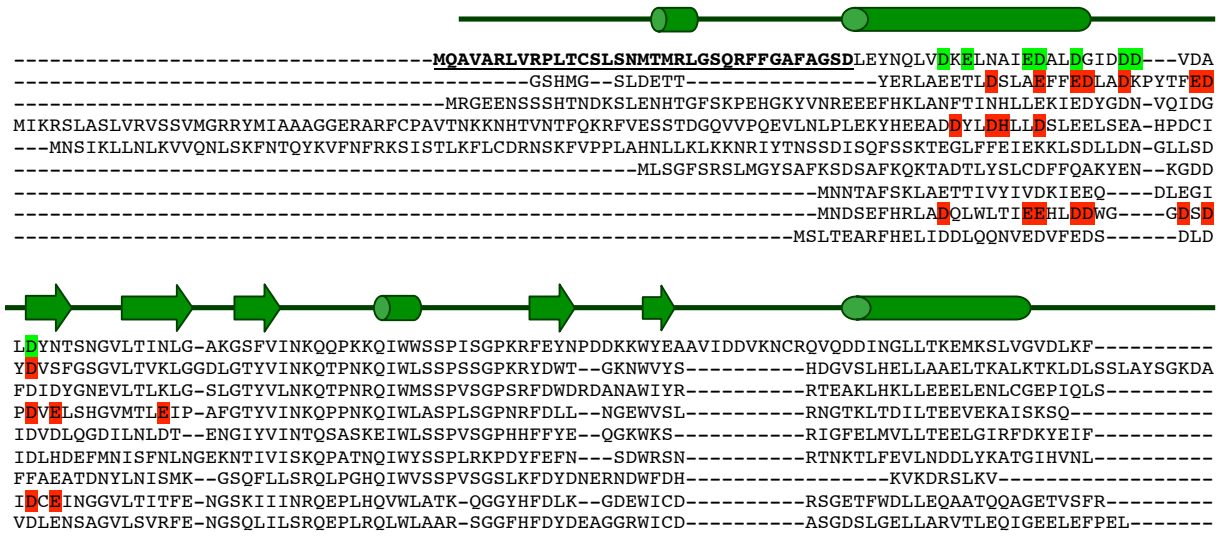

Fig S14

Conservation and identification of functional residues from cysteine desulphurase (IscS) of *Blastocystis*

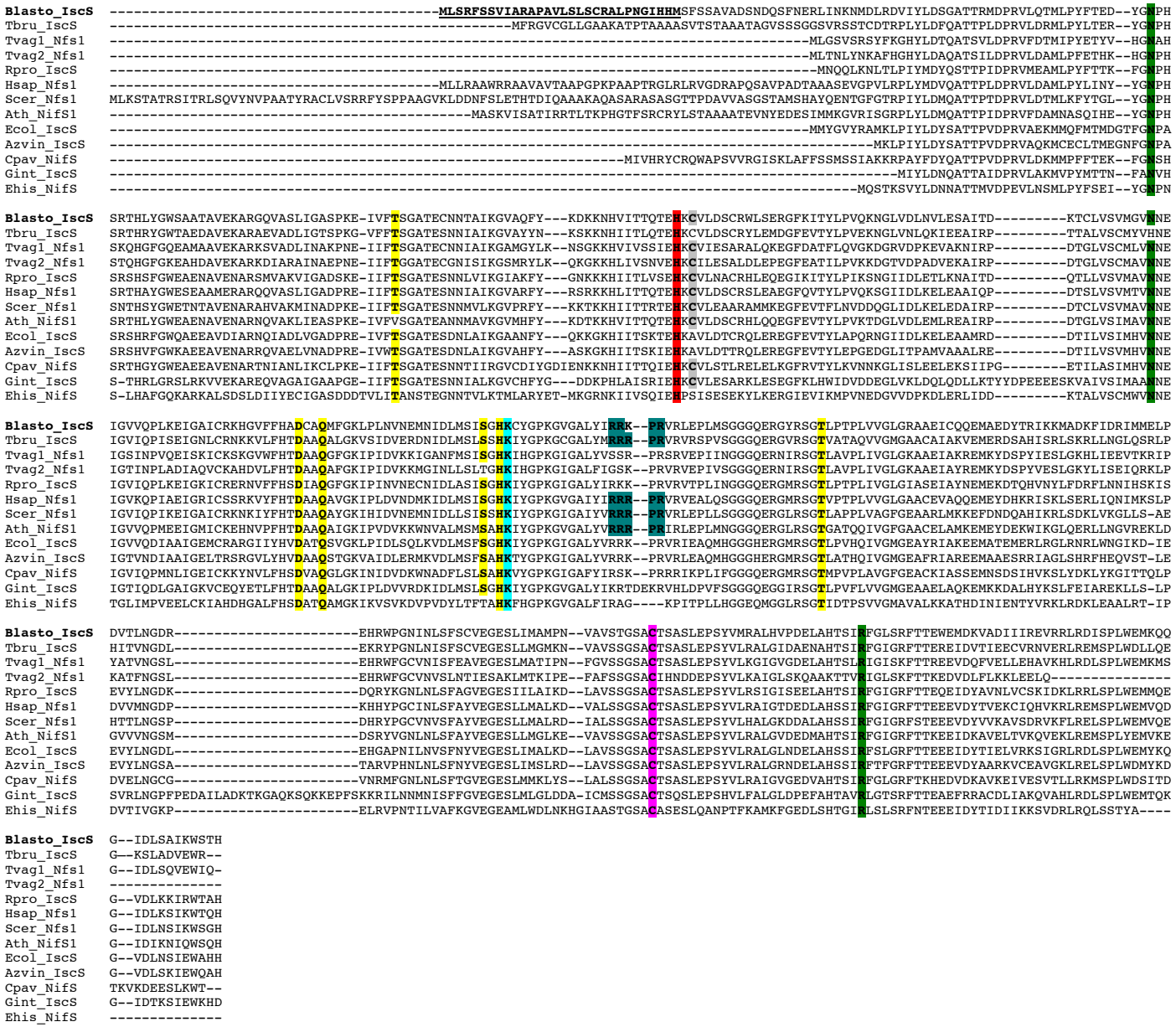

Fig S15

Conservation and Identification of functional residues of *Blastocystis* scaffold protein

Fig S16

a. *Bh*-Frataxin

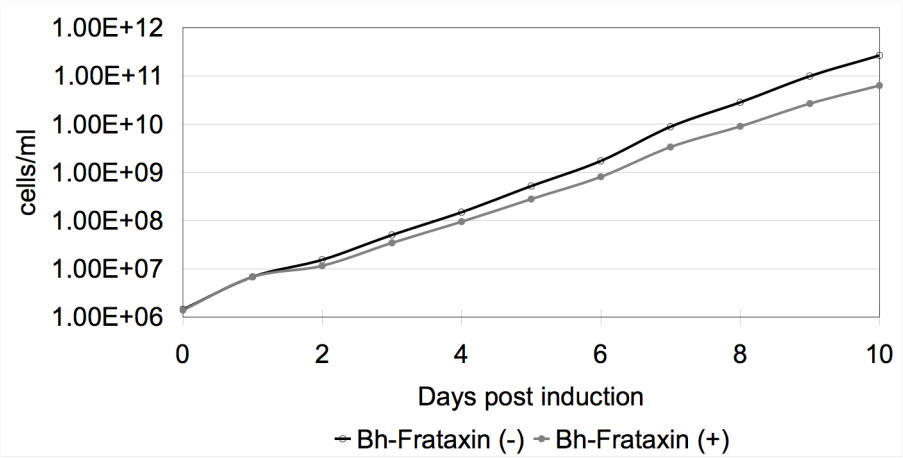

b. Frataxin KD

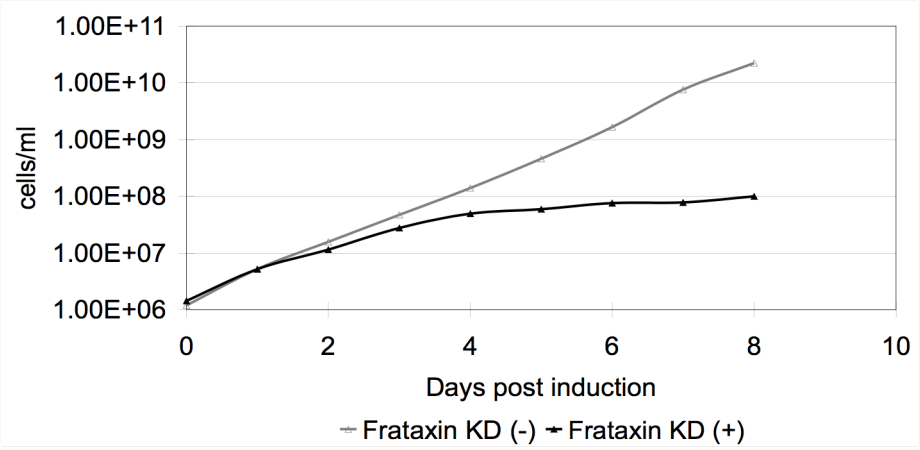

c. Frataxin KD + empty vector

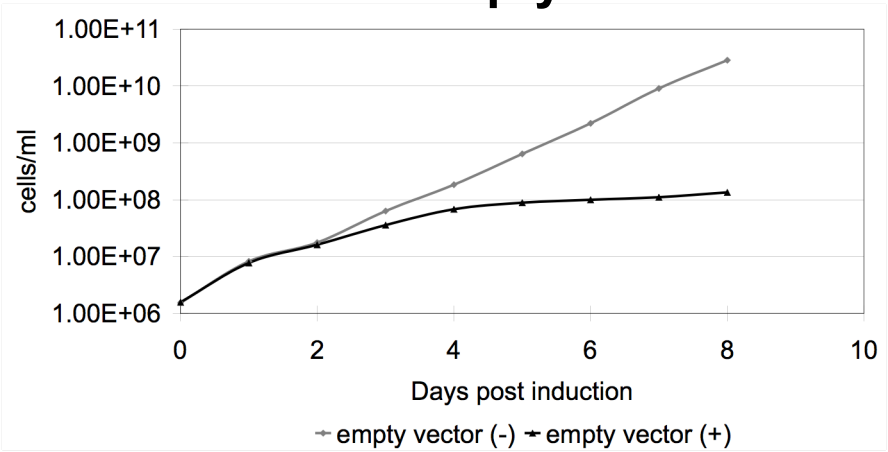

d. Fumarase

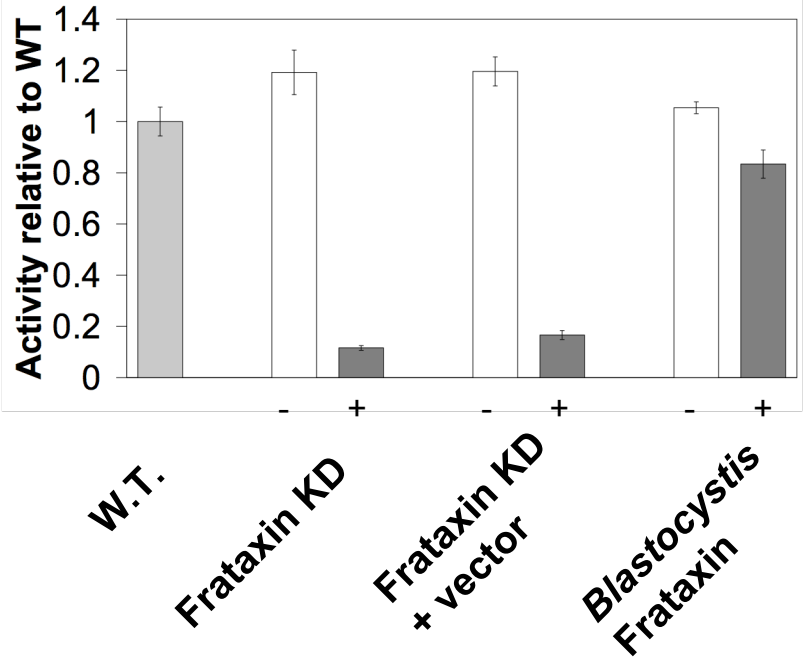

e. Aconitase

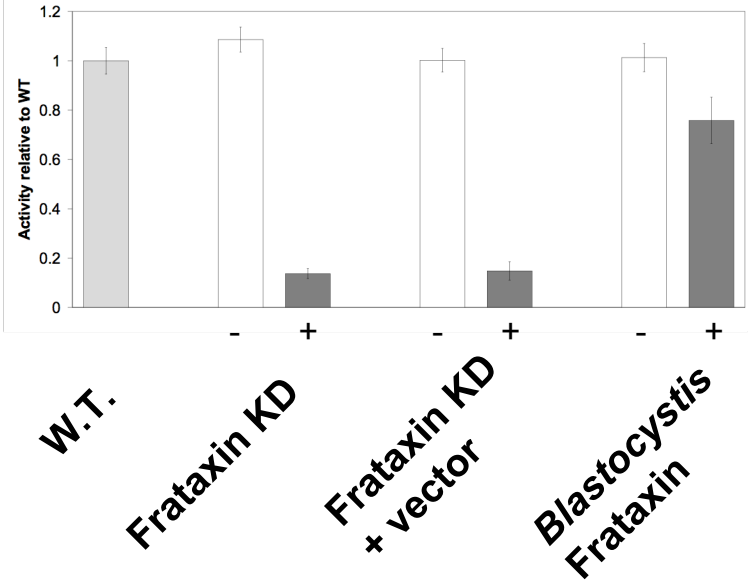

f. Threonine dehydrogenase

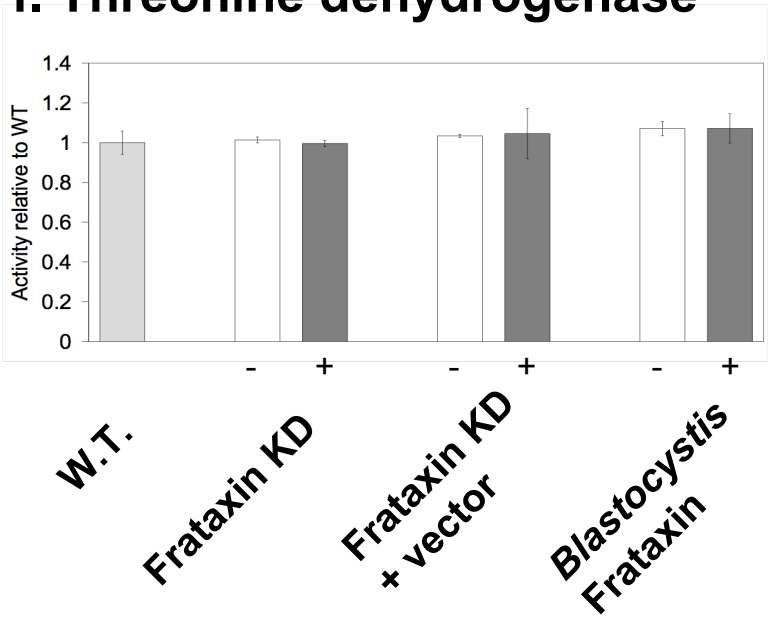

g. HA-tagged Frataxin

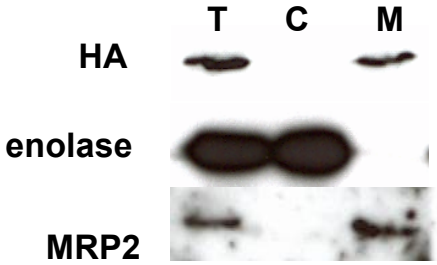

T: total protein extracts

C: Cytoplasm protein extracts

M: Mitochondrial protein extracts

HA: Frataxin fused with HA

Fig S17

a. *Bh*IscS & *Bh*IscS-*Ptr*Isd11

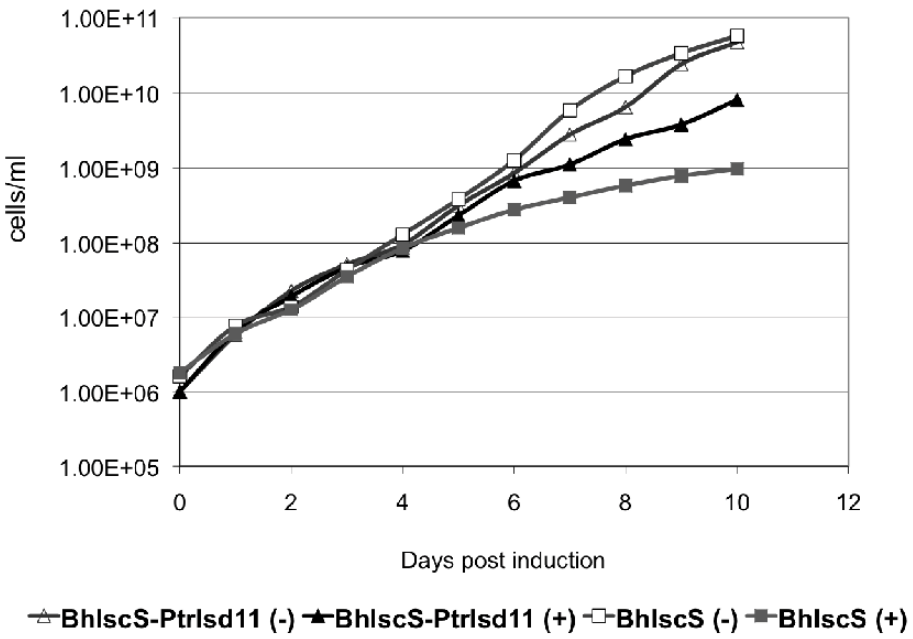

b. IscS Kd

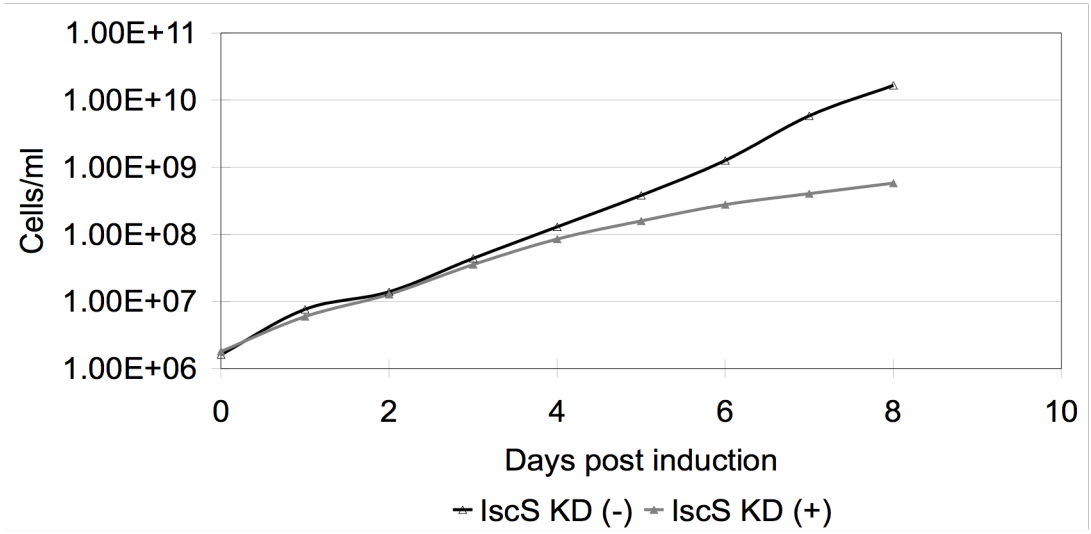

c. *Blastocystis* IscS + PCF vector

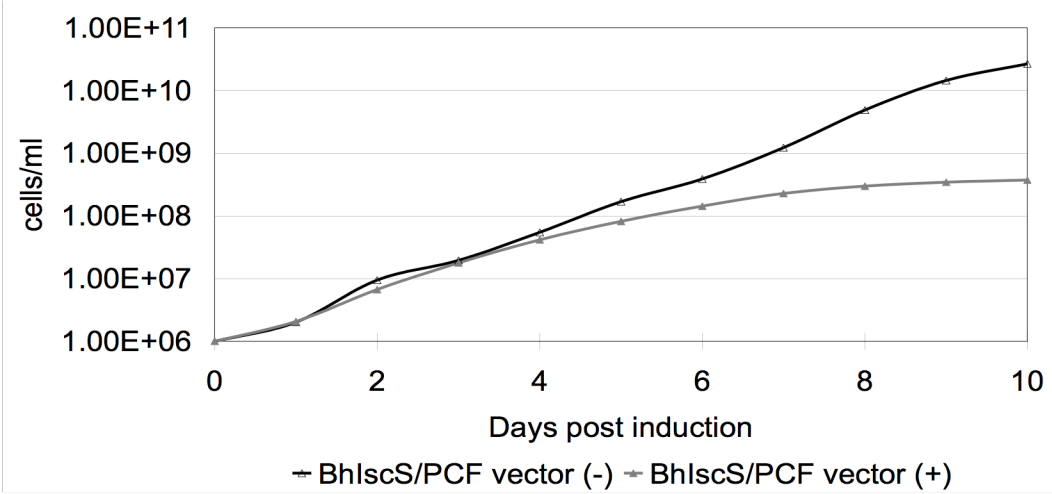

d. Aconitase

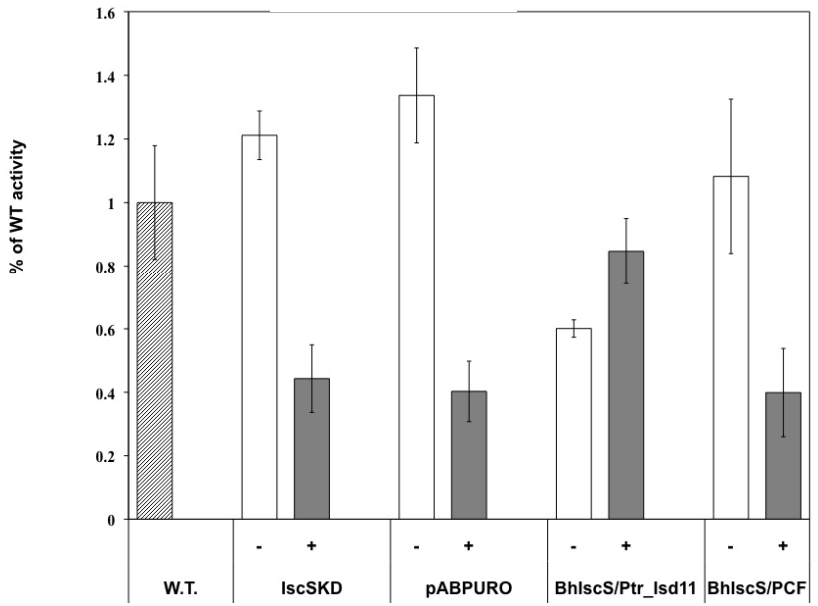

e. Succinate dehydrogenase

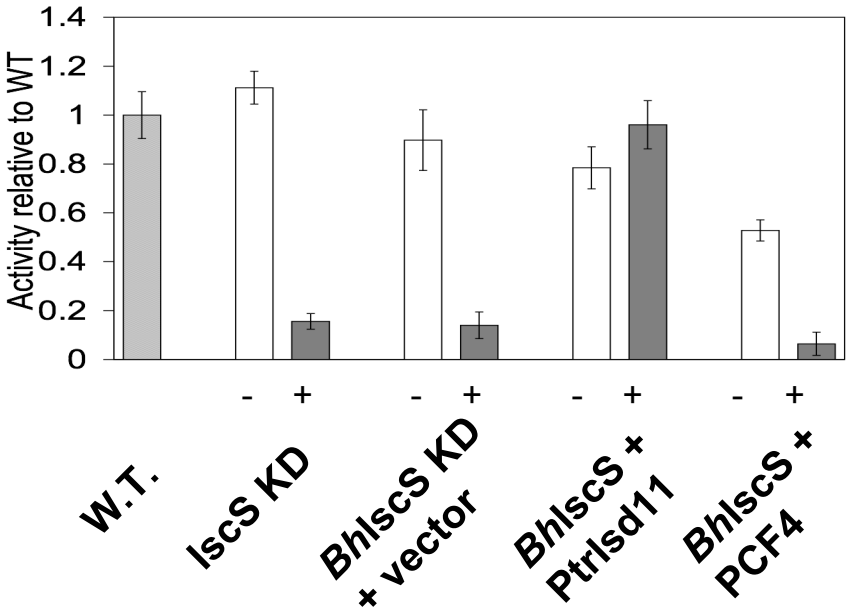

f. Threonine dehydrogenase

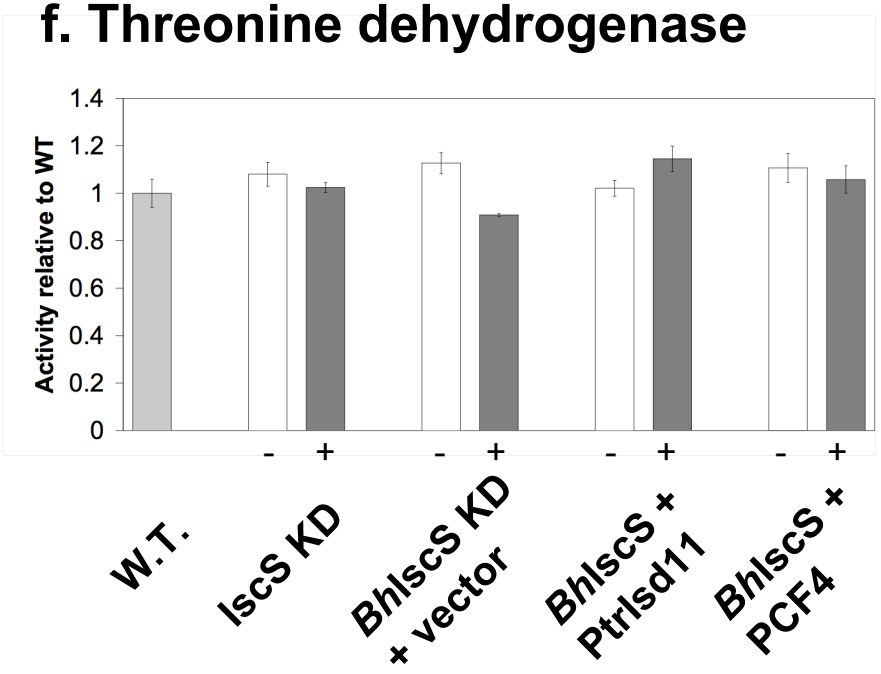

g. HA-tagged IscS

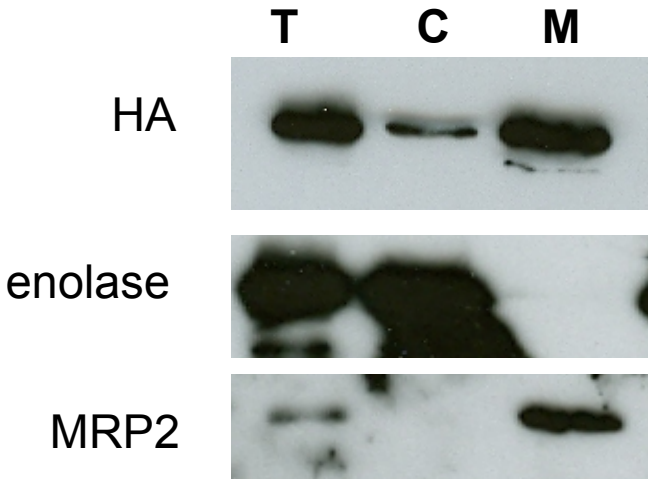

T: total protein extracts

C: Cytoplasm protein extracts

M: Mitochondrial protein extracts

HA: IscS fused with HA

Fig S18

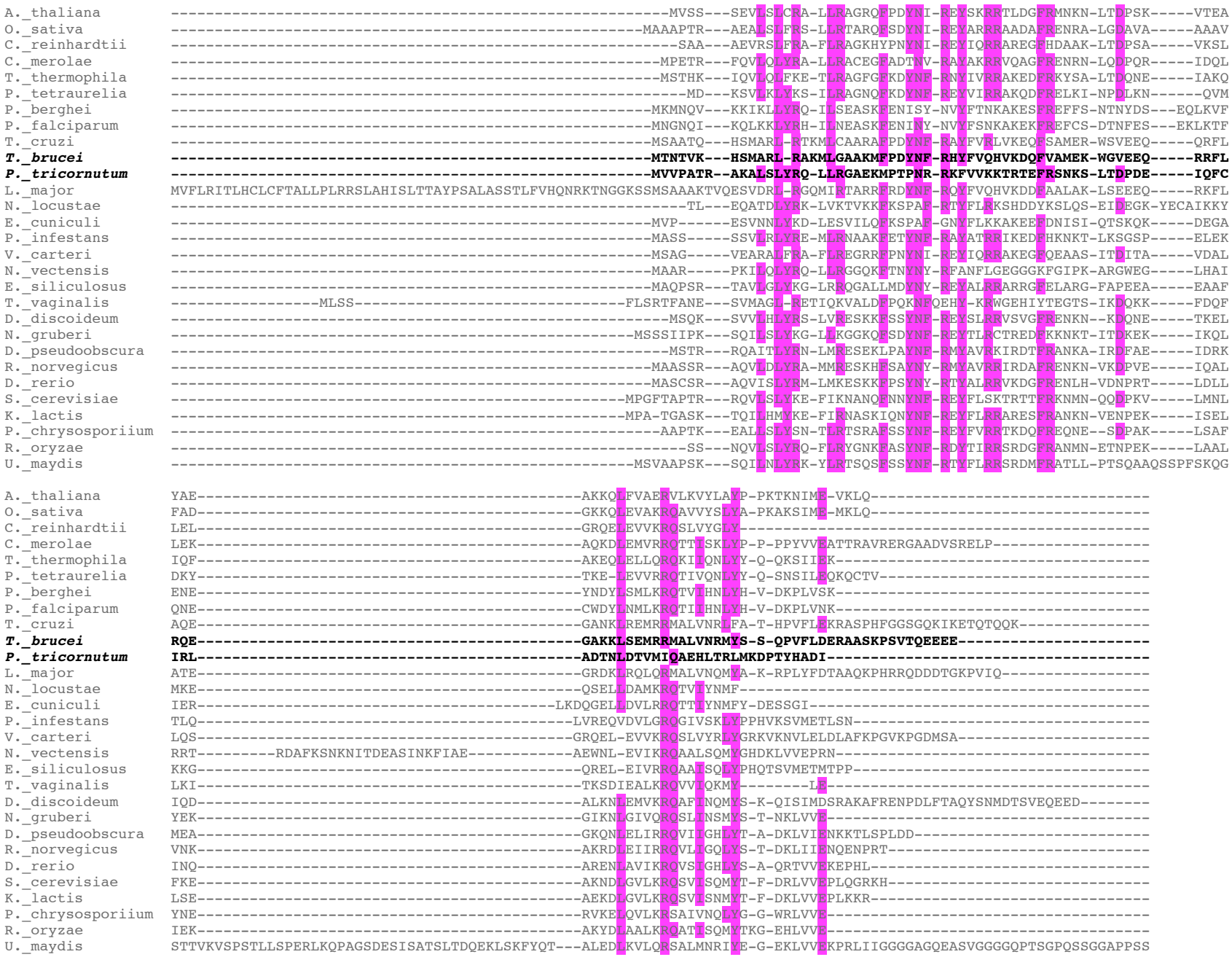
A._thaliana
O._sativa
C._reinhardtii
C._merolae
T._thermophila
P._tetraurelia
P._berghei
P._falciparum
T._cruzi
T._brucei
P._tricornutum
L._major
N._locustae
E._cuniculi
P._infestans
V._carteri
N._vectensis
E._siliculosus
T._vaginalis
D._discoideum
N._gruberi
D._pseudoobscura
R._norvegicus
D._rerio
S._cerevisiae
K._lactis
P._chrysosporiium
R._oryzae
U._maydis

Fig S19

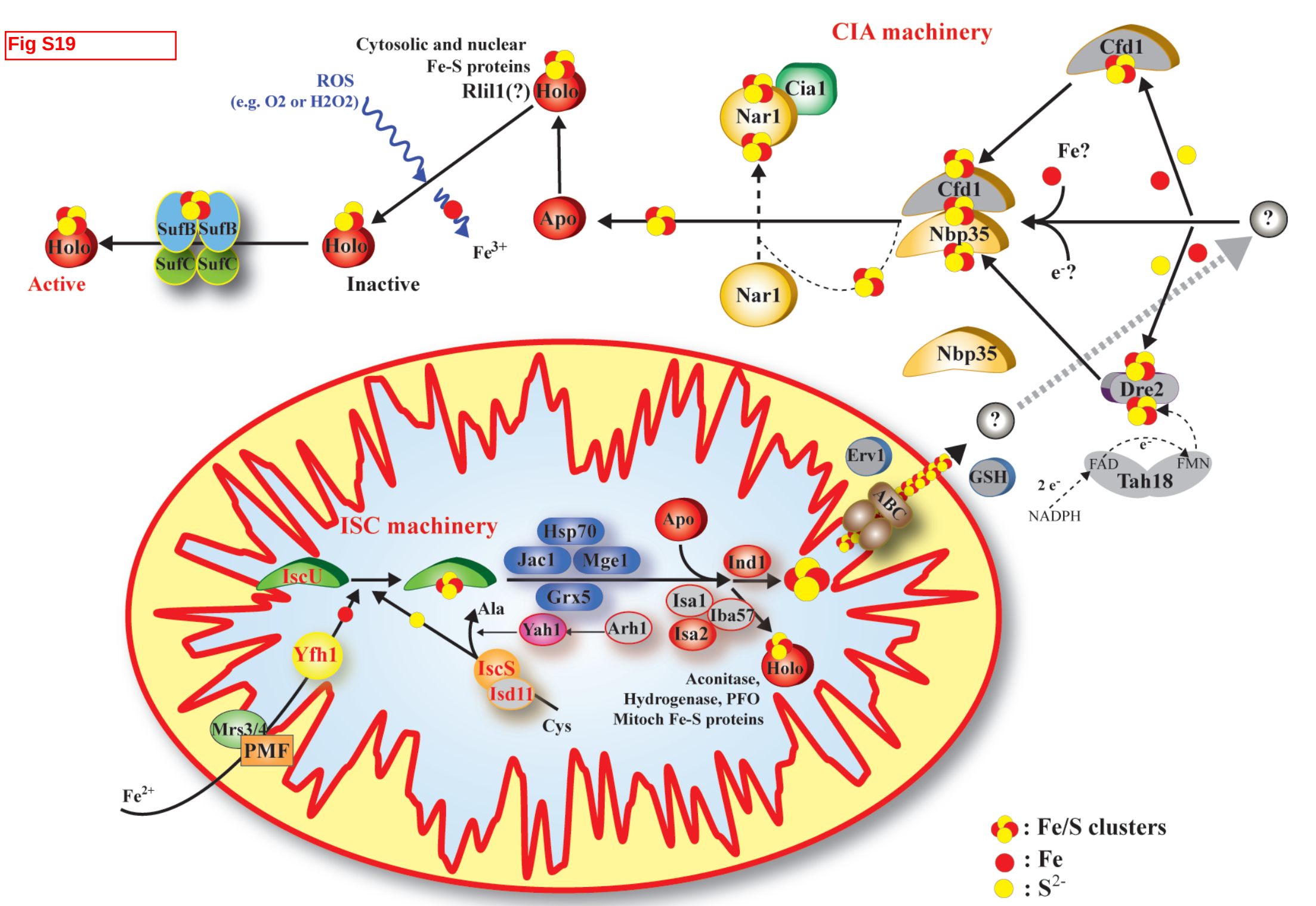
CIA machinery
Cytosolic and nuclear
Fe-S proteins
ROS
(e.g. O2 or H2O2)
Rlil1(?)
Holo
Cia1
Nar1
Cfd1
Fe?
Nbp35
e-?
?
Apo
Fe3+
SufB
SufC
Holo
Active
Inactive
Nbp35
Dre2
Erv1
ABC
GSH
FAD
FMN
Tah18
2 e-
NADPH
ISC machinery
Hsp70
Jac1
Mge1
Grx5
IscU
Ala
Yah1
Arh1
Isa1
Iba57
Isa2
Ind1
Yfh1
IscS
Isd11
Cys
Aconitase,
Hydrogenase, PFO
Mitoch Fe-S proteins
Mrs3/4
PMF
Fe2+
: Fe/S clusters
: Fe
: S2-

Fig S20

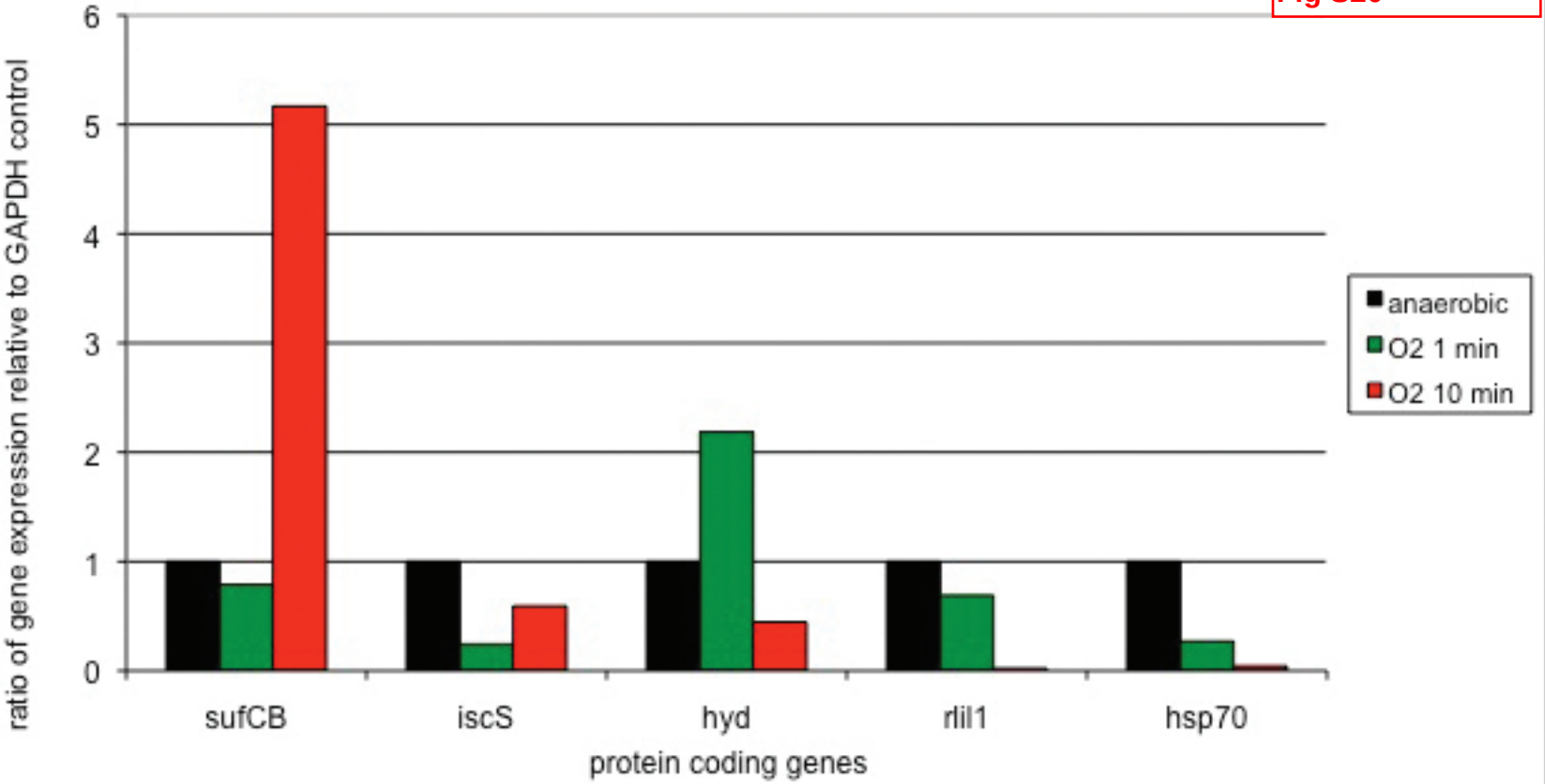
ratio of gene expression relative to GAPDH control
6
5
4
3
2
1
0
sufCB
iscS
hyd
rlil1
hsp70
protein coding genes
anaerobic
O2 1 min
O2 10 min

Fig S21

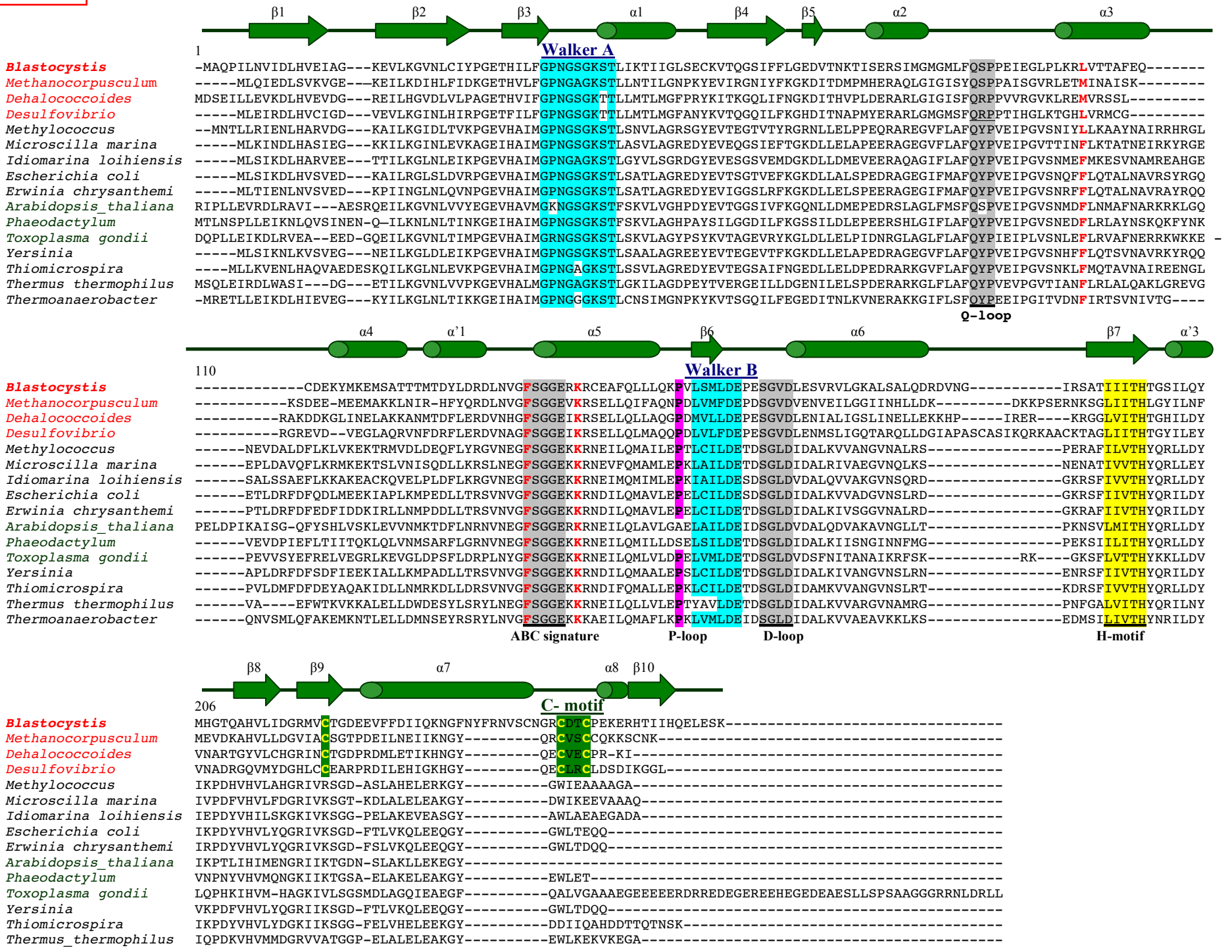
β1 β2 β3 α1 β4 β5 α2 α3
Walker A
Q-loop
α4 α'1 α5 β6 α6 β7 α'3
Walker B
ABC signature
P-loop
D-loop
H-motif
β8 β9 α7 α8 β10
C- motif
Blastocystis
Methanocorpusculum
Dehalococcoides
Desulfovibrio
Methylococcus
Microscilla marina
Idiomarina loihiensis
Escherichia coli
Erwinia chrysanthemi
Arabidopsis_thaliana
Phaeodactylum
Toxoplasma gondii
Yersinia
Thiomicrospira
Thermus thermophilus
Thermoanaerobacter

Fig S22

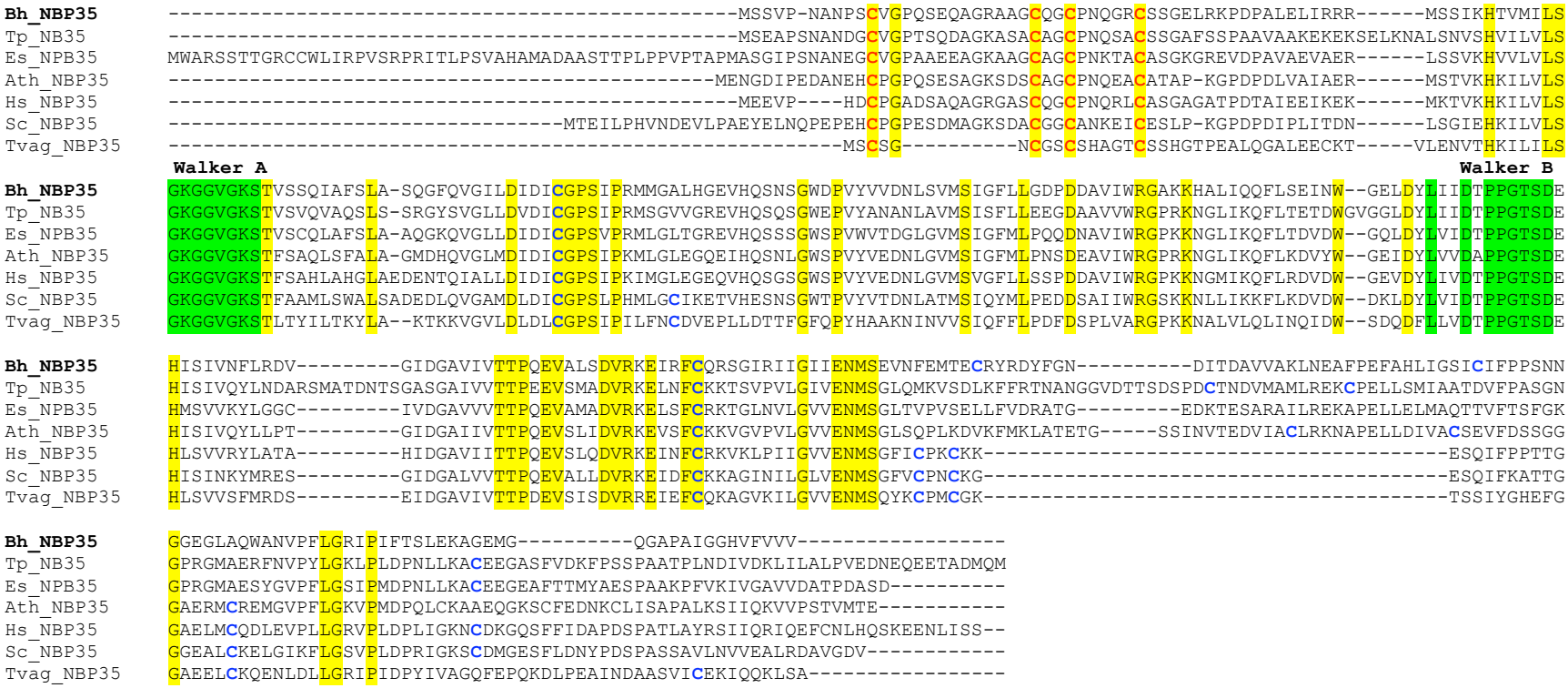
Bh_NBP35
Tp_NB35
Es_NPB35
Ath_NBP35
Hs_NBP35
Sc_NBP35
Tvag_NBP35
Walker A
Walker B

Table S1: Analyses of protein sequences involved in Fe-S cluster biogenesis using mitochondrial prediction programs

Proteins	Accession number	Mitopred	Mitoprot	Predotar	TargetP	Prediction of Signal peptide
ISC machinery						
IscU (ISU)	JN399203	0.99	0.9826	0.86	0.898	MYALTRSVSRLGVVARSLQCSSRFY
IscS (Nfs1)	JN399204	0.99	0.9703	0.47	0.787	MLSRFSSVIARAPAVLSLSCRALPNGIHHM
Frataxin (Yfh1)	JN399205	0.99	0.9921	0.65	0.903	MQAVARLVRPLTCSLSNMTMRLGSQRFFGAFAGSD
IscA (ISA)	JN399207	0.769	0.9949	0.9	0.907	MFRFSSALVRNALPSLTRARPAVSPLCSSLRLLSTEAKEA
mtHsp70	JN399206	0.99	0.9969	0.52	0.905	MNFISRVARSGMRSSLATLARTHMRT
Yah1 (1)	JN399208	0.846	0.9844	0.9	0.82	MLALRRLTPCVSKATNAVAARFISWTGKAA
Yah1 (3b11)	JN399209	0.846	0.9603	0.57	0.673	MLSIRGLFTVAKPLVSRSFVTIHFYT
Yah1 (8b10)	JN399210	0.769	0.9809	0.78	0.713	MAFLLRSVPLLTKRTCYPVFTRQFGVEFKLH
Mge1	JN399214	0.99	0.8934	0.65	0.935	MNRILTLGFRQSRMVLSSRALPCVNLIPASRAFHSSPFLF
Grx5	JN399212	0	0.6673	0.01	0.366	MKNYSRFPRVFFSSQSVD
Mrs3/4	JN399215	0	0.099	0	0.083	-
ISC export						
ATM1	JN399216	0	0.025	0.01	0.016	-
SUF machinery						
SufCB	JN399211	0	0.0661	0	0.055	-
CIA machinery						
Nbp35	JN399213	0.692	0.1606	0	0.096	-
Mitochondrial Fe/S proteins						
Hydrogenase	ACD10930	0.923	0.9304	0.91	0.831	MLSRLSRIATTKSMLVMNAARSFAAEAQGK
PFO	ACD10931	0.99	0.988	0.89	0.863	MFNTLVKRAMTSAARYNSVCAATLPKAVIARN

RED: Positive charged
Blue: Hydrophobic

Table S2: List of primers used in this project

Primer's name	**Primer sequence (5' => 3')**	**Gene**	**Reason**
BhFrat_ClaI_F	GGGCCCATCGATATGCAGGCGGTGGCACGATTGG	*frataxin*	cloning in pABPURO
BhFrat_HindIII_R	CGCGCGAAGCTTTTAGAATTTGAGACTAACGCCC	*frataxin*	cloning in pABPURO
BhFrat_HindIIIb_R	CGCGCGAAGCTTGAATTTGAGATCAACGCCCACC	*frataxin*	cloning in pABPURO-HA3
BhIscU_ClaI_F	GGGCCCATCGATATGTATGCATTAACCAGATCGGTG	*iscU*	cloning in pABPURO
BhIscU_HindIII_R	CGCGCGAAGCTTTTACTTTGACTTCTTTTCGCTCTTC	*iscU*	cloning in pABPURO
BhIscU_HindIIIb_R	CGCGCGAAGCTTCTTTGACTTCTTTTCGCTCTTC	*iscU*	cloning in pABPURO-HA3
BhIscS_ClaI_F	GGGCCCATCGATCTCTCCCGATTTAGCAGTGTG	*iscS*	cloning in pABPURO
BhIscS_HindIII_R	CGCGCGAAGCTTTTAATGGGTGCTCCACTTGATCG	*iscS*	cloning in pABPURO
BhIscS_HindIIIb_R	CGCGCGAAGCTTATGGGTGCTCCACTTGATCGCG	*iscS*	cloning in pABPURO-HA3
PtIsd11_HindIII_F	CGCGCGAAGCTTATGGTCGTACCTGCCACCCGAGC	*isd11*	cloning in PFC4
PtIsd11_BamH1_R	GGGCCCGGATCCTTATATGTCGGCATGATACGTTGG	*isd11*	cloning in PFC4
BhSufC_NdeI_F	CCCGGGCATATGGCGCAGCCTATTTTGAACGTTATTG	*sufCB*	cloning in pET16b
BhSufC_XhoI_R	GCGCGCCTCGAGTCAGAACCCCTCCTTGCTCGCC	*sufCB*	cloning in pET16b